Journal of Hazardous Materials 476 (2024) 134926

Contents lists available at ScienceDirect

Journal of Hazardous Materials

journal homepage: www.elsevier.com/locate/jhazmat

Compound- and element-specific accumulation characteristics of persistent toxic substances and metals in sediments of the Yellow Sea

Youngnam Kim [a], Yeonjung Lee [b], Chang-Eon Lee [c,d], Hyeryeong Jeong [c,e], Kongtae Ra [c], Donghan Choi [b], Seongjin Hong [a,d,*]

[a] Department of Earth, Environmental & Space Sciences, Chungnam National University, Daejeon 34134, Republic of Korea
[b] Ocean Climate Response & Ecosystem Research Department, Korea Institute of Ocean Science and Technology, Busan 49111, Republic of Korea
[c] Marine Environment Research Department, Korea Institute of Ocean Science and Technology, Busan 49111, Republic of Korea
[d] Department of Marine Environmental Sciences, Chungnam National University, Daejeon 34134, Republic of Korea
[e] Ifremer, CCEM-Unité Contamination Chimique des Ecosystèmes Marins (CCEM), F-44300, Nantes, France

HIGHLIGHTS

- The distribution of PTSs and metals in sediments exhibited a compound-specific manner.
- PCBs, styrene oligomers, and alkylphenols were accumulated near their sources.
- PAHs, originating from fossil fuel combustion, mainly accumulated in CYSM.
- Metals accumulated in CSYM similarly to PAHs and showed a grain size-dependent trend.
- The fate of PTSs was dependent on partition coefficients, such as log K_{OW} and log K_{OA}.

GRAPHICAL ABSTRACT

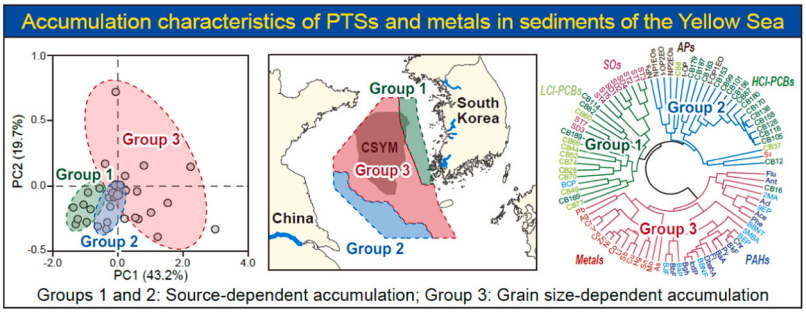

ARTICLE INFO

Keywords:
Yellow Sea
Sediments
Persistent toxic substances
Potential toxic elements
Source identification

ABSTRACT

This study investigated the large-scale distributions of persistent toxic substances (PTSs) and heavy metals in sediments of the Yellow Sea, collected from six transects between latitudes 32 and 37 degrees north (n = 35). Elevated concentrations of polychlorinated biphenyls (PCBs) were detected near the mainland, with a predominance of low-chlorinated congeners (di to tetra, ~60%), indicative of atmospheric deposition. Analysis of traditional and emerging polycyclic aromatic hydrocarbons (t-PAHs and e-PAHs) revealed notable enrichment in the Central Yellow Sea Mud Zone (CYSM), attributing fossil fuel combustion as the significant source. Styrene oligomers and alkylphenols exhibited notable accumulation near the Han River Estuary in South Korea and the Yangtze River Estuary in China, respectively. The accumulation of heavy metals was predominantly observed in the CYSM, with element-specific distribution patterns. Cluster analysis revealed distinct distribution patterns for PTSs and metals, highlighting their source-dependent and grain size-dependent behaviors. In addition, the distribution and accumulation of PTSs tended to depend on their partitioning coefficients, such as the octanol-air partition coefficient (log K_{OA}) and octanol-water partition coefficient (log K_{OW}). This study offers valuable insights into the sources, transport, and fate of hazardous substances in the Yellow Sea, emphasizing the necessity for targeted environmental management strategies.

* Corresponding author at: Department of Earth, Environmental & Space Sciences, Chungnam National University, Daejeon 34134, Republic of Korea.
E-mail address: hongseongjin@cnu.ac.kr (S. Hong).

https://doi.org/10.1016/j.jhazmat.2024.134926
Received 9 March 2024; Received in revised form 1 May 2024; Accepted 13 June 2024
Available online 19 June 2024

1. Introduction

Anthropogenic pollutants are a global concern, as evidenced by numerous studies. The rapid advancements in technology and industry in recent decades have led to expanding industrial complexes and urban areas along coastal regions [1]. This geographical placement results in a significant influx of hazardous substances from human activities into marine environments via water and atmospheric transport [2]. Persistent toxic substances (PTSs) and heavy metals, known for their environmental persistence and resistance to degradation, are capable of long-range transport in marine settings [3,4]. Their high particle adsorption capacity leads to accumulation in sediments, negatively impacting marine ecosystems by harming benthic organisms or reintroducing pollutants into the water column through resuspension [5,6]. While much research has focused on pollutant distribution and sources within harbors, rivers, estuaries, and coastal areas directly linked to human activities [7], there is growing recognition of the presence and effects of PTSs and metals in less disturbed environments like regional seas, oceans, and polar regions [8,9]. Regional seas, acting as connectors between the coast and the open ocean, are crucial for understanding the long-range transport of hazardous substances, yet research in these domains remains scarce.

The Yellow Sea is one of the large marine ecosystems. It is surrounded by South Korea, China, and North Korea and is subject to pollution stress from all three countries. The Yellow Sea, characterized by its shallow depth of approximately 100 m, is bordered by the East Asian continent, the Korean Peninsula, and Japan, forming a semi-enclosed basin [10]. Major urban centers across different countries surround this region, hosting significant populations and industrial complexes within metropolitan areas [11]. Additionally, it receives considerable inputs of terrestrial substances from prominent rivers such as the Yellow River, Huai River, Yangtze River, and Han River. Positioned in the mid-latitudes, the Yellow Sea is subjected to a substantial influx of atmospheric and particulate matter from the land, largely driven by seasonal monsoons [10]. The water circulation of the Yellow Sea is predominantly counterclockwise, centered around its basin [12]. This circulation pattern facilitates the deposition of terrestrial substances in the central region, known as the Central Yellow Sea Mud (CYSM), where a significant accumulation of sediments occurs [13]. The CYSM is notably characterized by a high proportion of settled materials, playing a pivotal role in the distribution of various compounds within the sediments of the Yellow Sea [14].

The sedimentation characteristics of the Yellow Sea influence the distribution of PTSs and heavy metals [15]. Furthermore, PTSs and metals can exhibit different distributions based on their physicochemical properties [16,17]. For instance, the mobility and sedimentation of metals in marine environments are affected by variables such as suspended particulate matter, pH, and salinity, which can alter the forms of the metals and dictate their long-range transportability and deposition mechanisms [18,19]. Similarly, the distribution and mobility of PTSs are influenced by their molecular mass and partitioning coefficients, such as the octanol-water partition coefficient (K_{OW}) and octanol-air partition coefficient (K_{OA}). In previous studies, compounds with high K_{OW} values, such as polychlorinated biphenyls (PCBs), tended to accumulate near pollution sources, whereas compounds with low K_{OW} values, such as styrene oligomers (SOs) and alkylphenols (APs), were transported farther through ocean currents [20-22]. The adsorption of pollutants onto suspended particles may vary with changes in salinity, potentially affecting their ability to travel long distances [23]. Some studies have reported that the accumulation of PTSs can occur irrespective of specific physicochemical properties, such as organic carbon (OC) content and grain size [24]. The source of PTSs and metals are often linked to similar anthropogenic activities, including industrial processes, steel production, and coke manufacturing [25-27]. Analyzing distribution patterns and similarities using various indicators such as environmental factors, metals, and PTSs can be advantageous for elucidating the pathway and fate of numerous compounds [28]. However, accurate comparisons are challenging due to the limited data on various compounds. Thus, understanding the transport and accumulation patterns of pollutants in marine settings is essential for revealing the complex processes governing the dispersal of these harmful substances.

This study aims to elucidate the spatial distributions of PTSs and metals in surface sediments of the Yellow Sea, identify potential sources, and determine accumulation mechanisms. The investigation mapped the pollutant distribution across a wide geographic area, spanning latitudes 32 to 37 degrees north. The target analytes were selected to encompass various sources and a wide range of physicochemical properties, including a total of 71 PTSs [32 PCBs, 15 traditional polycyclic aromatic hydrocarbons (t-PAHs), 8 emerging PAHs (e-PAHs), 10 SOs, and 6 APs] and 17 heavy metals (Mn, Li, V, Cr, Co, Ni, Cu, Zn, As, Sr, Mo, Ag, Cd, Sn, Sb, Pb, and Hg). The study area includes the Korea-China Interim Measures Zone, and such large-scale monitoring efforts have rarely been conducted; thus, the data will be valuable for future assessment of national pollution contributions and management of the Yellow Sea ecosystem.

2. Materials and methods

2.1. Study area and sampling

Field investigation and sample collection were conducted during a cruise of the R/V Onnuri (KIOST, Korea) in May 2021. Surface sediments (0–2 cm) were collected from 35 sites, with latitude intervals of 1 degree ranging from 32 degrees to 37 degrees north, using a Smith-McIntyre Grab (Fig. 1 and Table S1). Sediments were collected for analysis of sediment grain size, organic carbon (OC), total nitrogen (TN), and carbon and nitrogen stable isotopes ($\delta^{13}C$ and $\delta^{15}N$), PTSs, and heavy metals, and stored at −20 ℃. The sediments were freeze-dried, and impurities were removed using a 2-mm sieve.

2.2. Sediment grain size analysis

The sediment samples were treated with 30% hydrogen peroxide and 1 M hydrochloric acid to remove organic matter and carbonate minerals. After the acid treatments, samples were analyzed using an alternative laser-based method with a Mastersizer 2000 (Malvern Instruments, Ltd., Worcestershire, UK) [29].

2.3. Organic carbon, total nitrogen, and stable isotopes analysis

For quantification of organic carbon (OC) and carbon stable isotopes, approximately 1 g of freeze-dried sediment was treated with 1 M hydrochloric acid to eliminate inorganic carbon. Following the removal, distilled water was added to neutralize the acid, and centrifugation was employed to separate and remove the supernatant. Subsequently, freeze-drying was performed. OC and $\delta^{13}C$ were measured using an elemental analyzer (EA; Vario ISOTOPE cube, Elementar, Hanau, Germany) coupled with IRMS (Isoprime VisION, Elementar, Manchester, UK). Total nitrogen (TN) content and nitrogen stable isotopes were analyzed without pretreatment. The isotopic ratios ($\delta^{13}C$ and $\delta^{15}N$) were calculated using the following Eq. (1).

$$\delta\ ^{13}C \text{ or } \delta^{15}N\ (‰) = [(R_{sample}/R_{standard}) - 1] \times 1000 \quad (1)$$

Vienna Pee Dee Belemnite (VPDB) was employed as the reference material for carbon isotopic analysis, and atmospheric nitrogen isotopic composition was used as the reference for nitrogen isotopic analysis. The analytical accuracy for $\delta^{13}C$ and $\delta^{15}N$ was found to be within 0.05 ‰ and 0.07 ‰, respectively.

2.4. Persistent toxic substances analysis

The analysis procedure for determining PTSs in sediments followed the previous studies [30,31]. Approximately 10 g of homogenized sediments were filled into a stainless-steel cell with a filler and extracted using an accelerated solvent extractor (Dionex ASE 350, Thermo Scientific, Salt Lake City, UT) at 100 ℃ for 15 min with dichloromethane (DCM, Burdick & Jackson, Muskegon, MI). Surrogate standards were added before extraction to assess extraction efficiency. The extracts were then replaced with hexane (Burdick & Jackson), and samples were concentrated to 1 mL using a nitrogen gas concentrator (TurboVap LV, Biotage, Uppsala, Sweden). Activated copper powder (Merck, Darmstadt, Germany) was added to react for 1 h, removing elemental sulfur. Purification and fractionation were carried out using silica gel (70–230 mesh, Sigma-Aldrich, Saint Louis, MI) column chromatography. The first fraction (F1) was eluted with 30 mL of hexane for PCBs, and the second fraction (F2) was eluted with 60 mL of hexane:DCM (4:1, v/v) for analysis of PAHs and SOs. The final fraction (F3) was eluted with 50 mL of DCM:acetone (3:2, v/v) for APs analysis. All eluents were concentrated to 1 mL, and 100 ng of 2-fluorobiphenyl (ChemService, West Chester, PA) was added as an internal standard. Instrumental analysis was conducted using gas chromatography (Agilent 7890B GC, Agilent Technologies, Santa Clara, CA) coupled with a 5977B mass selective detector (MSD, Agilent Technologies). Detailed information regarding target compounds, detection limits, recovery, and instrument conditions for PTSs analysis is provided in Tables S2 and S3.

2.5. Principal component analysis with multiple linear regression

The principal component analysis coupled with multiple linear regression (PCA-MLR) was used to quantitatively assess the source contributions of PAHs [32]. In this study, concentrations of 15 PAHs, excluding naphthalene, were utilized as the primary dataset across 35 sampling sites. To determine the source factors of PAHs, PCA was conducted with varimax rotation and Kaiser normalization. Only factors with eigenvalues greater than or equal to 1 were considered as principal components [33]. The adequacy of the PCA was confirmed by the Kaiser-Meyer-Olkin (KMO) test, which yielded a value exceeding 0.05.

2.6. Heavy metals analysis

Homogenized sediment samples were digested using a mixture of hydrofluoric, nitric, and perchloric acid (5:4:1; Suprapur®, Merck) for 24 h at 180 °C. Subsequently, after drying, dissolution was carried out using 1% (v/v) nitric acid. The concentrations of metals were measured using an inductively coupled plasma-mass spectrometry (ICP-MS; iCAP Q, Thermo Fisher Scientific, Bremen, Germany). The mercury (Hg) concentration was measured using an automated direct Hg analyzer (Hydra-C, Teledyne Leeman Labs Inc., Hudson, NH) without pretreatment. MESS-4 (National Research Council, Ottawa, ON, Canada) was used as a certified reference material for accuracy assessment. The accuracy of the measured concentrations of 17 metals relative to the certified concentrations was within satisfactory ranges of 93.8–99.0% for all elements.

2.7. Enrichment factor calculation

To mitigate variations stemming from weathered sediment and estimate the human impact, the enrichment factor (EF) is commonly employed, utilizing a normalization element, such as Al or Fe [34]. This method is utilized to account for the effects of heterogeneous sediments. Background concentrations of heavy metals in the Yellow Sea were referenced from a previous study [35]. EF values were calculated using the following Eq. (2).

$$EF = (M/Al)_S/(M/Al)_R \quad (2)$$

Where M and Al represent the concentrations of the respective metal and aluminum, S denotes the observed value, and R signifies the reference sample. EF values below 1 are generally considered non-enriched, primarily attributed to crustal contributions [36]. Values in the range of 1.0–1.5 indicate influx due to anthropogenic activities or external sources.

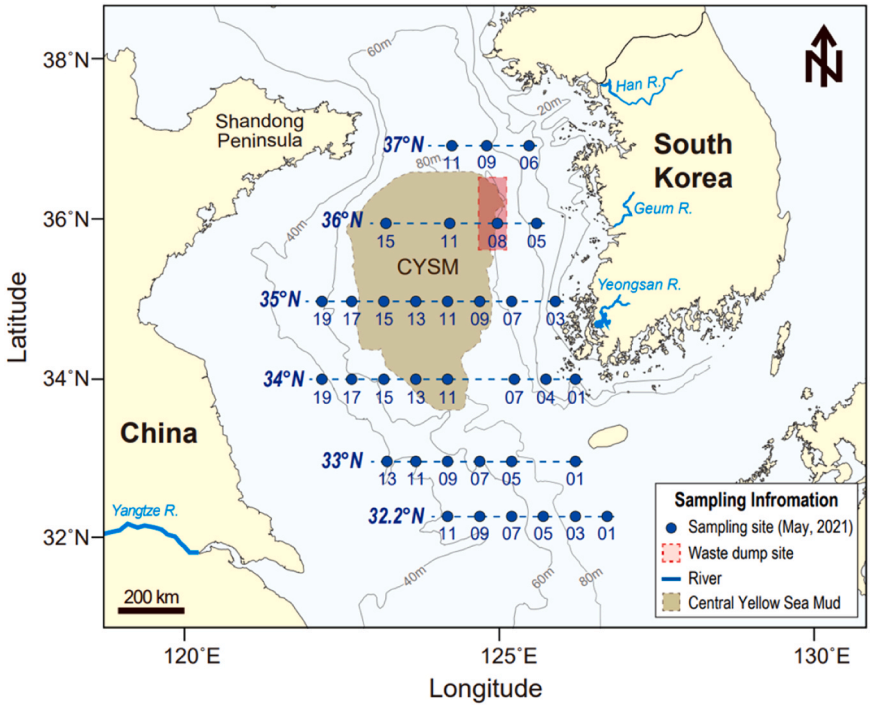

Fig. 1. Map showing the sampling sites in the Yellow Sea. A total of thirty-five surface sediments (0–2 cm) were collected in May 2021 (CYSM: Central Yellow Sea Mud; Red dotted boxes: waste dump site).

2.8. Statistical analysis

PCA and cluster analysis were employed to elucidate the distribution trends of environmental variables, metals, and organic pollutants. PCA was performed using SPSS 26 (SPSS Inc., Chicago, IL), and cluster analysis was conducted using R software (Version 4.0.2). The varimax method was utilized for PCA, and the KMO test indicated a statistically significant basis for the analysis, with a result exceeding 0.5. Spearman's rank correlation analysis was conducted using R software to examine the similarity among sediment properties, concentrations of heavy metals, and PTSs.

3. Results and discussion

3.1. General characteristics of sediments in the Yellow Sea

The spatial distribution of sediment grain size, OC, TN, and stable isotope ratios in the Yellow Sea are shown in Fig. 2 and Table S1. The mean grain size ranges from 7.1 to 290 μm (1.8–7.1 Ø), indicating a markedly diverse grain size distribution in the Yellow Sea. Coastal regions generally exhibited greater grain sizes, while the area around 37 degrees north of the Korean Peninsula and adjacent locations demonstrates a course grain size (Fig. 2a). Notably, at 37 degrees north, a higher proportion of sand is evident compared to other regions. This distinctive grain size distribution is characteristic of the northeastern Yellow Sea, which is primarily composed of erosive sandy deposits formed during the last stages of the glacial period [37]. Moreover, it is presumed that grain size distribution has been significantly influenced by substantial inflows of terrestrial substances from the Shandong Peninsula and the Han River [38]. Across the range of 34–36 degrees north, a substantial area known as the CYSM was identified in the central part, where the silt content exceeded 70%, with an increasing clay content [39]. This grain size distribution is attributed to counter-clockwise currents along the coast of the Yellow Sea, causing smaller particles, which are relatively lighter and can remain suspended for longer durations, to accumulate in the central part of the Yellow Sea [40].

The OC contents in sediments of the Yellow Sea ranged from 0.1% to 1.1%, with an average of 0.45%, while the TN contents ranged from 0.02% to 0.18%, averaging at 0.08% (Fig. 2b). In comparison to adjacent seas, such as the Bohai Sea and the East China Sea, the Yellow Sea exhibited relatively low OC contents [41,42]. The spatial distribution of OC in the Yellow Sea revealed a higher concentration in the central part, similar to the distribution of silt and clay [43]. This suggests that the accumulation of OC is influenced by its adsorption onto fine sediments, such as silt and clay contents.

The $\delta^{13}C$ values in surface sediments of the Yellow Sea ranged from –23.3 ‰ to –20.7 ‰, with an average of –21.6 ‰. The region between latitudes 32 and 34 degrees north exhibited a heavier $\delta^{13}C$ than the area between latitudes 35 and 37 degrees north (Fig. 2c). Although marine organic matter typically demonstrates a heavier isotopic composition around –20.0 ‰ of $\delta^{13}C$ [44], the relatively lighter isotopic composition observed in the 35 to 37-degree north region suggests a distinct origin of organic matter in the southern Yellow Sea and CSYM [45]. Lighter $\delta^{13}C$ values indicate the influence of terrestrial-derived substances or exhibit characteristics found in aged sediments or those near adjacent continents [46,47]. Additionally, when pico-sized phytoplankton become dominant in the water column due to environmental changes, $\delta^{13}C$ values in particulate organic matter may exhibit lighter values [48,49]. The relatively lighter $\delta^{13}C$ values in CSYM compared to the southern part may also be influenced by artificial organic matter, reflecting complex influences from the crust or organisms [50].

3.2. Distributions and sources of persistent toxic substances in sediments of the Yellow Sea

3.2.1. Polychlorinated biphenyls

The concentrations of PTSs in sediments of the Yellow Sea have been normalized by OC contents to account for regional variations [51]. The levels of PCBs in sediments ranged from 42 to 1300 ng g^{-1} OC, with an average of 350 ng g^{-1} OC (Table S4). The spatial distributions of PCBs in sediments of the Yellow Sea revealed relatively higher concentrations in areas adjacent to large rivers, such as the Han River and the Yangtze River (Fig. 3a). The composition of PCBs was predominantly low-chlorinated PCBs (di- to tetra-CBs; LCl-CBs) in the overall Yellow Sea region, but the relative proportion of high-chlorinated PCBs (penta- to hepta-CBs; HCl-CBs) increased in some southwestern areas of the Yellow Sea (Fig. S1 and Table S4). The high proportion of LCl-CBs is associated with combustion sources, while the HCl-CBs are assumed to be product sources [52]. PCA was conducted to assess the potential sources of PCBs using the compositions of PCBs in sediments obtained from this study and those of potential sources reported previously (Fig. S2). To partially account for compositional fractionation based on molecular mass and the number of chlorines in the environment, PCA was performed using existing data from coastal areas of China and Korea [30,53]. The results of the PCA showed that PCBs composition of the Yellow Sea sediments was similar to that of the Yangtze River Estuary and the west coast of Korea, indicating combustion sources. Thus, it suggests that PCBs are produced through combustion processes, introduced into the environment through rivers and atmospheric deposition, and accumulate in the coastal areas of Korea and China. In particular, HCl-CBs with relatively low mobility accumulated in areas near the sources, while LCl-CBs with high mobility were transported far away and accumulated in the central Yellow Sea (Fig. S1). South Korea banned

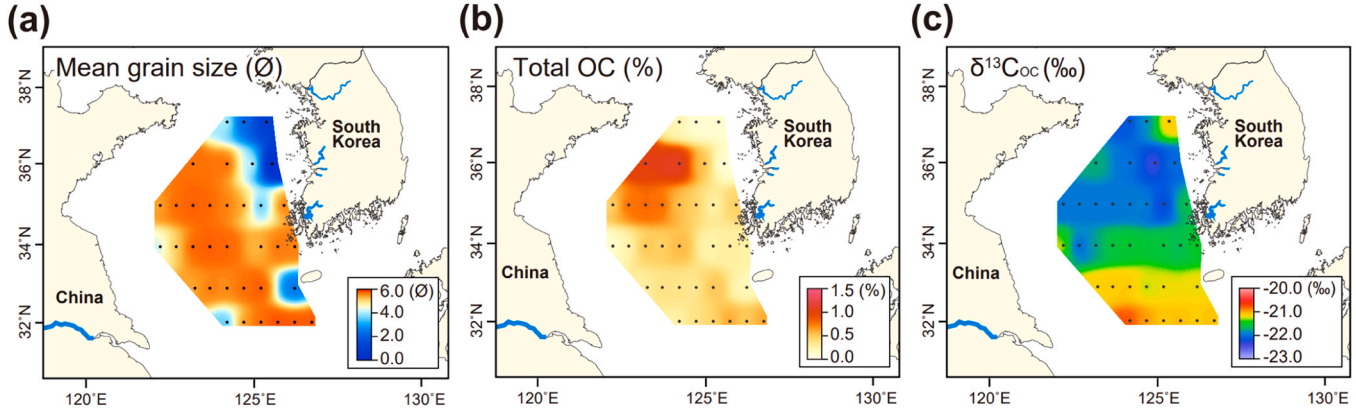

Fig. 2. Distributions of **(a)** mean grain size (Φ), **(b)** organic carbon contents (%), and **(c)** carbon stable isotope ratios ($\delta^{13}C$, ‰) of organic carbons in sediments of the Yellow Sea.

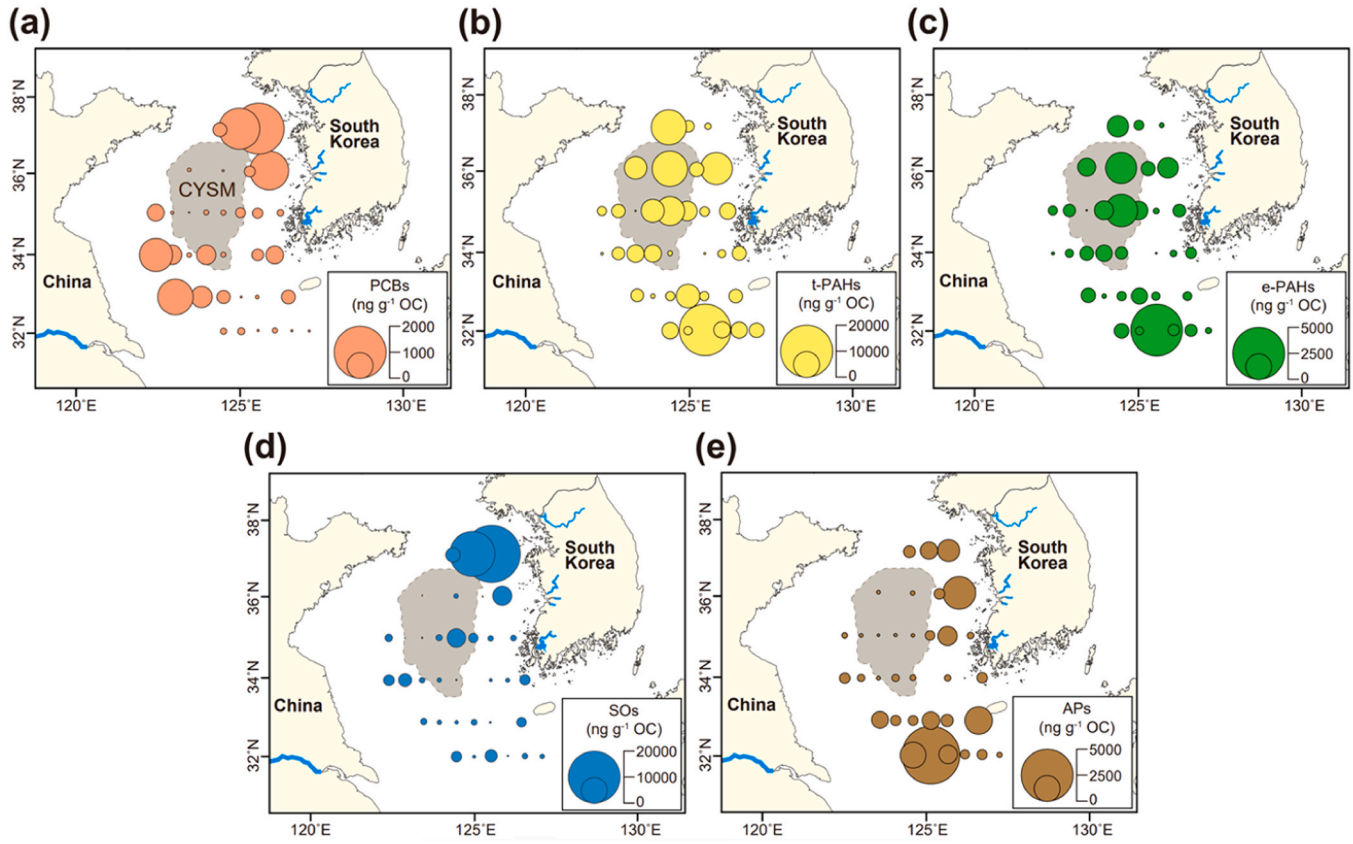

Fig. 3. Spatial distributions of **(a)** PCBs, **(b)** traditional PAHs (t-PAHs), **(c)** emerging PAHs (e-PAHs), **(d)** SOs, and **(e)** APs in sediments of the Yellow Sea. The concentrations of PTSs were normalized using the organic carbon contents of the sediments.

the use of PCBs in 1979, and China joined the Stockholm Convention in 2004, implementing regulations [30,54]. Currently, PCBs from unintended byproducts dominate the Yellow Sea region compared to those derived from products.

3.2.2. *Traditional and emerging polycyclic aromatic hydrocarbons*

The concentrations of traditional polycyclic aromatic hydrocarbons (t-PAHs) and emerging polycyclic aromatic hydrocarbons (e-PAHs) in sediments of the Yellow Sea ranged from 570 to 17,000 ng g^{-1} OC and from 160 to 4500 ng g^{-1} OC, respectively (Tables S5 and S6). t-PAHs are prioritized for management by the USEPA, and e-PAHs denote compounds with similar molecular structures and toxicity to t-PAHs but are currently unmanaged. Both t-PAHs and e-PAHs, exhibiting similar physicochemical properties, showed comparable spatial distributions (r^2 =0.89, $p < 0.01$) [55]. Relatively elevated concentrations of PAHs were observed in the CYSM region, as well as near Korea and in the central part of 32 degrees north latitude (Figs. 3b and 3c). The coast of South Korea is known for industrial activities associated with PAHs, such as coke production [56]. The central part of 32 degrees north latitude shows relatively high concentrations as terrestrial substances from the Yangtze River tend to accumulate due to changes in water depth caused by the continental shelf [57]. The distributions of PAHs, OC, and grain size were similar, indicating that PAHs appear to behave similarly to the deposition of suspended particles and OC in the Yellow Sea [58]. Unlike PCBs, PAHs are found to transport to distant areas in the Yellow Sea environment rather than accumulating near the sources. The composition of PAHs in the Yellow Sea was mainly dominated by 3-ring PAHs, with sediments in the CSYM also exhibiting relatively high concentrations of 4-ring PAHs (Fig. S1). The high proportion of 3–4 ring PAHs is known to be associated with anthropogenic activities, including fossil fuel combustion and the steel industry [59]. The predominance of 3-ring PAHs entering the aquatic environment is thought to be due to their relatively long half-life and strong long-distance mobility compared to other compounds [60]. PCA-MLR was employed to identify potential sources of PAHs in the Yellow Sea (Fig. 4). The sources attributed to the Yellow Sea were identified as vehicle emissions, fossil fuel combustion, and coke production [61,25,26]. The relatively high contribution of coke production near South Korea is thought to impact the region, primarily distributed along the western coast of Korea [56]. Great contributions of fossil fuel combustion and vehicle emission sources were prevalent in most regions. PAHs are thought to be adsorbed on suspended particles, transported long distances, and ultimately deposited in the central Yellow Sea. However, in marine environments, the composition of PAHs can change during transport by the influence of environmental factors, making it difficult to identify the source of pollution accurately [62]. Further research on the method applied in this study is needed; carbon and hydrogen stable isotope ratios of individual PAHs have more conservative characteristics and can be used to identify sources [63].

3.2.3. *Styrene oligomers*

Concentrations of SOs in sediments ranged from 340 to 25,000 ng g^{-1} OC, with an average of 4000 ng g^{-1} OC (Table S7). Concentrations of SOs were ten to hundreds of times higher in sites near the Han River compared to other regions (Fig. 3d). SOs are formed through the degradation of plastics and expanded polystyrene (EPS) products [64]. It is assumed to be introduced in significant quantities through the corrosion of plastics discharged via major cities, large rivers, and sources like nearby aquaculture facilities [64]. Regarding the composition of SOs, in the region close to the coastal area, styrene trimers (STs) accounted for a relatively high proportion compared to other regions, and the proportion of styrene dimers (SDs) was found to be relatively high as it moved toward the CSYM (Fig. S1). SDs are known to be by-products of STs, and the SDs/STs ratio increased toward the center

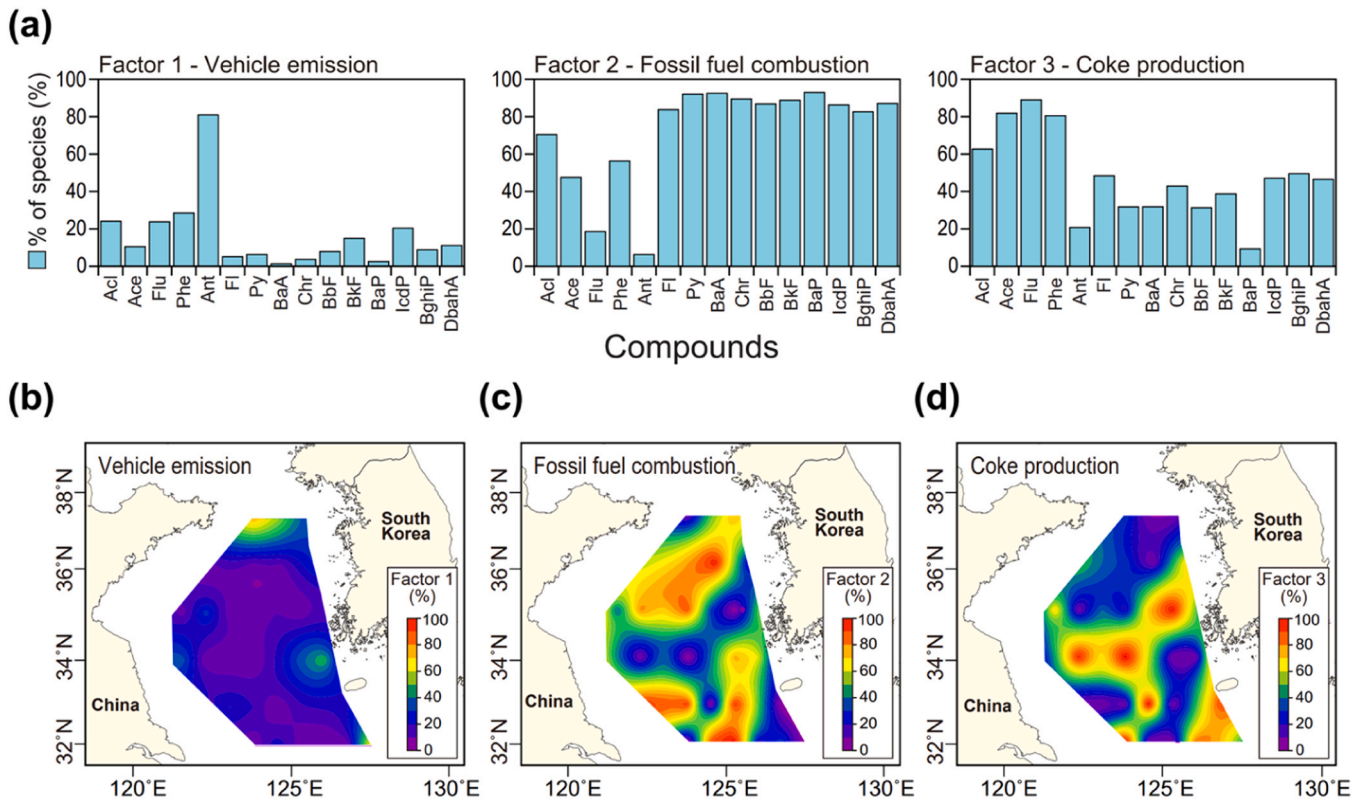

Fig. 4. **(a)** Three factors, such as vehicle emission, fossil fuel combustion, and coke production, were derived.
Source appointment of PAHs in sediments of the Yellow Sea using principal component analysis (PCA) with multiple linear regression (MLR). The contributions of **(b)** vehicle emission, **(c)** fossil fuel combustion, and **(d)** coke production sources to PAHs in sediments of the Yellow Sea were contour mapped.

of the Yellow Sea. Among the SOs, the ratio of ST1 to SD2 can be utilized to assess the continuous inflow of pollutants [65]. When using the diagnostic ratio, the Yellow Sea is identified as having residues of previously introduced compounds at most sampling points (Fig. S3). However, at sites N3706 and N3709, where high concentrations of SOs were observed, relatively low diagnostic ratios indicating recent influx were observed, similar to those at terrestrial-adjacent sites (i.e., N3302 and N3411). These results suggest that ongoing inputs have had some influence in those areas.

3.2.4. Alkylphenols

Concentrations of APs in sediments were found to range from 47 to 3800 ng g^{-1} OC, with an average of 820 ng g^{-1} OC (Table S8). The highest concentration of APs was detected in the southern part of the Yellow Sea, and relatively high concentrations were found at the sites near the west coast of South Korea (Fig. 3e). APs are degradation products of alkylphenol polyethoxylates, which have been used as detergents, wetting agents, and dispersing agents, and they are primarily transported through water [66]. In South Korea, APs have been banned since 2004, while in China, there is no regulation for the use of APs and related compounds. Due to this national difference in uses and management of compounds, relatively high concentrations of APs were detected near the Yangtze River [67]. Additionally, it has been observed that terrestrial-origin substances, organic pollutants, and heavy metals discharged from the Yangtze River are introduced into the Yellow Sea [68,69]. Due to differences in the flow of seawater caused by variations in continental shelf depths, many substances tend to accumulate in sediments. These environmental characteristics could be determining factors in the accumulation of organic pollutants [70]. Continuous pollution of APs can be assessed using the ratio of APs to the parent compounds (i.e., alkylphenol ethoxylates) in environmental samples [71,72]. Evaluation using nonylphenols and octylphenols and their ethoxylates ratios showed that the influx of fresh sources was dominant in most parts of the Yellow Sea (Fig. S3). In environments less impacted by human activities, such as offshore areas, NP ratios indicative of a fresh source indicate that NPs have low persistence in the environment and undergo significant degradation [73]. This finding is consistent with previous studies, highlighting the challenge of utilizing NP ratios in offshore environments [30].

3.3. Distributions and enrichment of heavy metals in sediments of the Yellow Sea

Concentrations of heavy metals in sediments of the Yellow Sea are shown in Fig. 5 and Table S9. Metals exist naturally in the environment and may also occur due to anthropogenic activities; among various metals, Hg, Cd, As, Cu, Pb, Li, Ni, Cr, V, and Zn are considered potential toxic elements (PTEs). Most PTEs exhibited high concentrations in the central region of the Yellow Sea, specifically in the CSYM (Fig. 5). Greater concentrations of Mo and Mn were observed in the northwest rather than the central part of the Yellow Sea. Cd and Ag showed relatively elevated concentrations not only in the central region of the Yellow Sea but also in the waste dump site of the West Sea, Korea. High concentrations of Co, Cr, and V were observed in all sites except the northeastern Yellow Sea, and exceptionally high concentrations of Sr were observed in the southeastern Yellow Sea. Sr is known to be an element that contributes to the formation of biological skeletons and shells, such as diatoms and clams [74]. There are many islands in areas with high Sr concentrations, and in particular, Jeju Island and nearby areas in Korea are greatly influenced by organisms due to the development of aquaculture.

Excluding Sr ($p > 0.05$), most heavy metals exhibited a strong positive correlation with sediment grain size and OC contents, while showing a significant negative correlation with sand contents (Table 1).

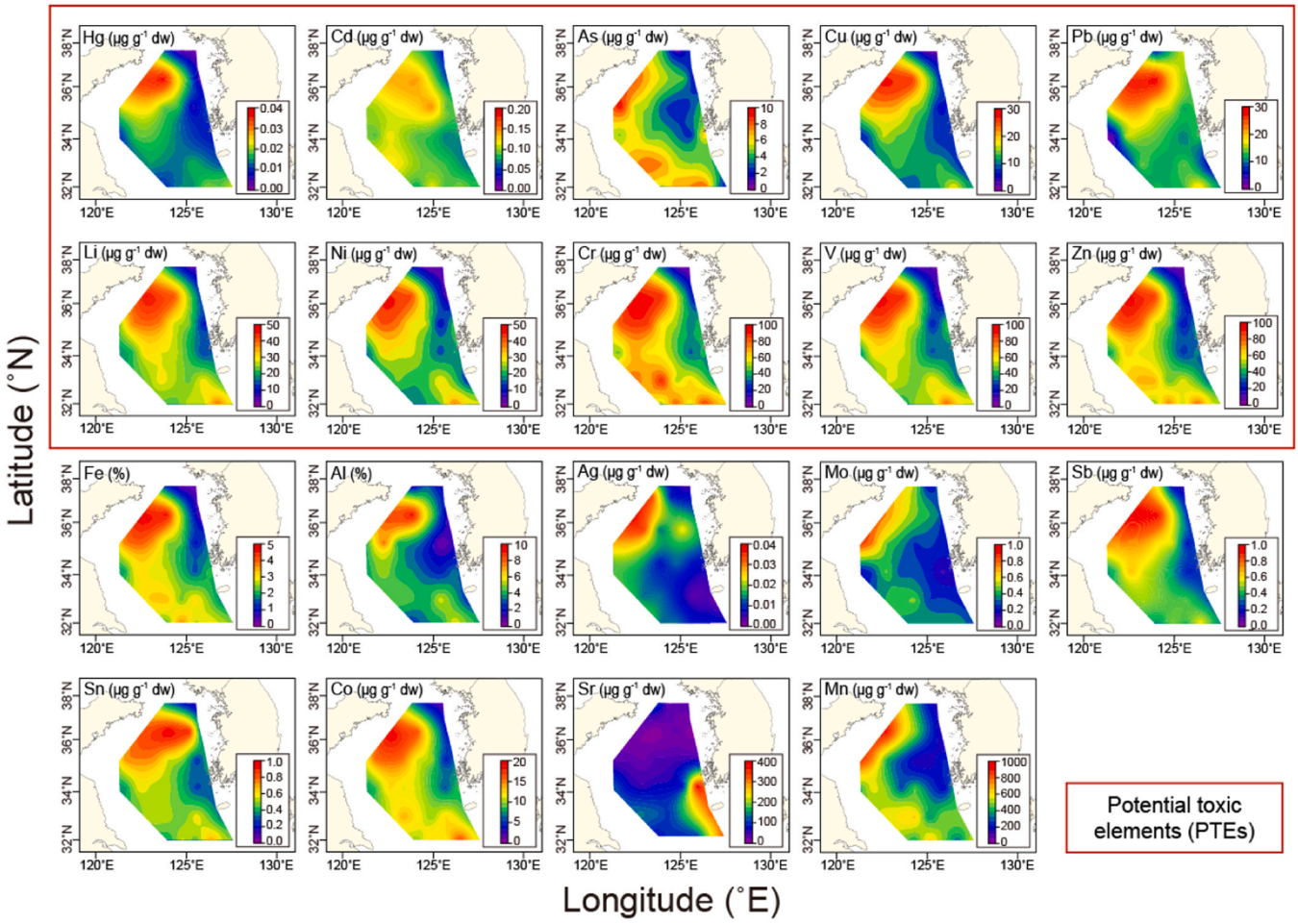

Fig. 5. Spatial distributions of the 10 potential toxic elements (Hg, Cd, As, Cu, Pb, Li, Ni, Cr, V, and Zn) and other metals (Fe, Al, Ag, Mo, Sb, Sn, Co, Sr, and Mn) in sediments of the Yellow Sea.

As widely acknowledged, the distribution of heavy metals in aquatic environments is highly correlated with grain size and organic matter [75]. Among the heavy metals, Mn and As showed relatively higher concentrations in the northwest rather than the central part of the Yellow Sea; unlike other heavy metals, they showed relatively low correlations with grain size and OC contents. The distribution of Mn and As in the Yellow Sea is likely influenced by both sedimentation and biological factors [76]. This fraction of Mn is prone to deposition in coarse sediment with high oxygen content, leading to the formation of MnO_2 [77]. Another mechanism that may have caused such distribution of Mn is likely due to the sediment in this high-content area being dominated by biogenic carbonate [78].

Since heavy metals are fundamental elements constituting the Earth's crust, to observe anthropogenic influences, it is necessary to eliminate the influence of background concentrations [79]. Co, Cu, Sn, and Hg were not enriched in surface sediments in the Yellow Sea, as their EF values did not exceed 1 (Table S10). Sr has been observed to be significantly enriched, with EF values exceeding 1.5, in the coastal areas of Jeju Island and the south coast of Korea. The southern part of the Korean Peninsula and Jeju Island are relatively shallow, with numerous islands in the study area known for abundant nutrients and active biological activities. Sr is widely recognized as a biological indicator in the

Table 1
Relationship between grain size and organic carbon contents and metals of surface sediments in the Yellow Sea.

Sediment property	Heavy metals																
	Mn	Li	V	Cr	Co	Ni	Cu	Zn	As	Sr	Mo	Ag	Cd	Sn	Sb	Pb	Hg
Grain size (Ø)	0.41*	0.84**	0.76**	0.75**	0.81**	0.79**	0.68**	0.81**	0.49**	0.16	0.31	0.35*	0.59**	0.63**	0.60**	0.40*	0.67**
Sand (%)	–0.47**	–0.92**	–0.81**	–0.79**	–0.87**	–0.87**	–0.78**	–0.89**	–0.53**	–0.10	–0.40*	–0.46**	–0.66**	–0.71**	–0.71**	–0.46**	–0.78**
Silt (%)	0.48**	0.91**	0.81**	0.79**	0.86**	0.86**	0.78**	0.88**	0.53**	0.09	0.41*	0.48**	0.67**	0.71**	0.72**	0.45**	0.77**
Clay (%)	0.31	0.85**	0.73**	0.72**	0.80**	0.80**	0.68**	0.82**	0.41*	0.14	0.28	0.25	0.46**	0.61**	0.57**	0.47**	0.67**
OC (%)	0.47**	0.92**	0.81**	0.79**	0.87**	0.87**	0.78**	0.89**	0.53**	0.10	0.40*	0.46**	0.66**	0.71**	0.71**	0.46**	0.78**

* $p < 0.05$
** $p < 0.01$

formation of shells and corals [80]. This outcome is likely attributed to biological influences from numerous islands and aquaculture activities along the southern coast of Korea [81]. Most heavy metals are enriched with EF values exceeding 1 in the central part of the Yellow Sea. This means that most metals exhibit distribution dependent on grain size and OC contents in the Yellow Sea. At the N3608 site, Ag and Cd exhibited EF values of 1, while other heavy metals showed EF values below 0.7. The relatively high EF values of Ag and Cd are thought to be influenced by the waste dump site [82].

3.4. Transport, fate, and accumulation of persistent toxic substances and heavy metals

In offshore environments, the deposition of heavy metals and PTSs is influenced by various environmental factors, including topography, hydrological conditions, grain size, OC content, geographical location, and proximity to pollution sources [83]. The study of the distribution and composition of PTSs and heavy metals in marine settings is crucial for understanding their patterns of fate and accumulation [84]. Spearman's rank correlation analysis was conducted to identify factors controlling the distributions of PTSs and metals (Fig. S4). In the Yellow Sea, there were no significant correlations between water depth and other sedimentary parameters, such as OC contents and grain size. In contrast, significant correlations were observed between grain size and OC contents. The carbon and nitrogen isotope ratios, which are indicative of the origin of organic matter, did not show a significant correlation with PTSs and metals. This is attributed to the complex influence on sedimentary organic carbon in the Yellow Sea, stemming from both allochthonous anthropogenic sources and autochthonous sources such as pico-sized phytoplankton [48]. The increase in surface area due to the decrease in grain size provides adsorption sites for organic matter, organic pollutants, and heavy metals; consequently, smaller grain sizes typically correspond to higher concentrations of OC and pollutants [85,86].

The distributions of heavy metals, including PTEs, exhibited a

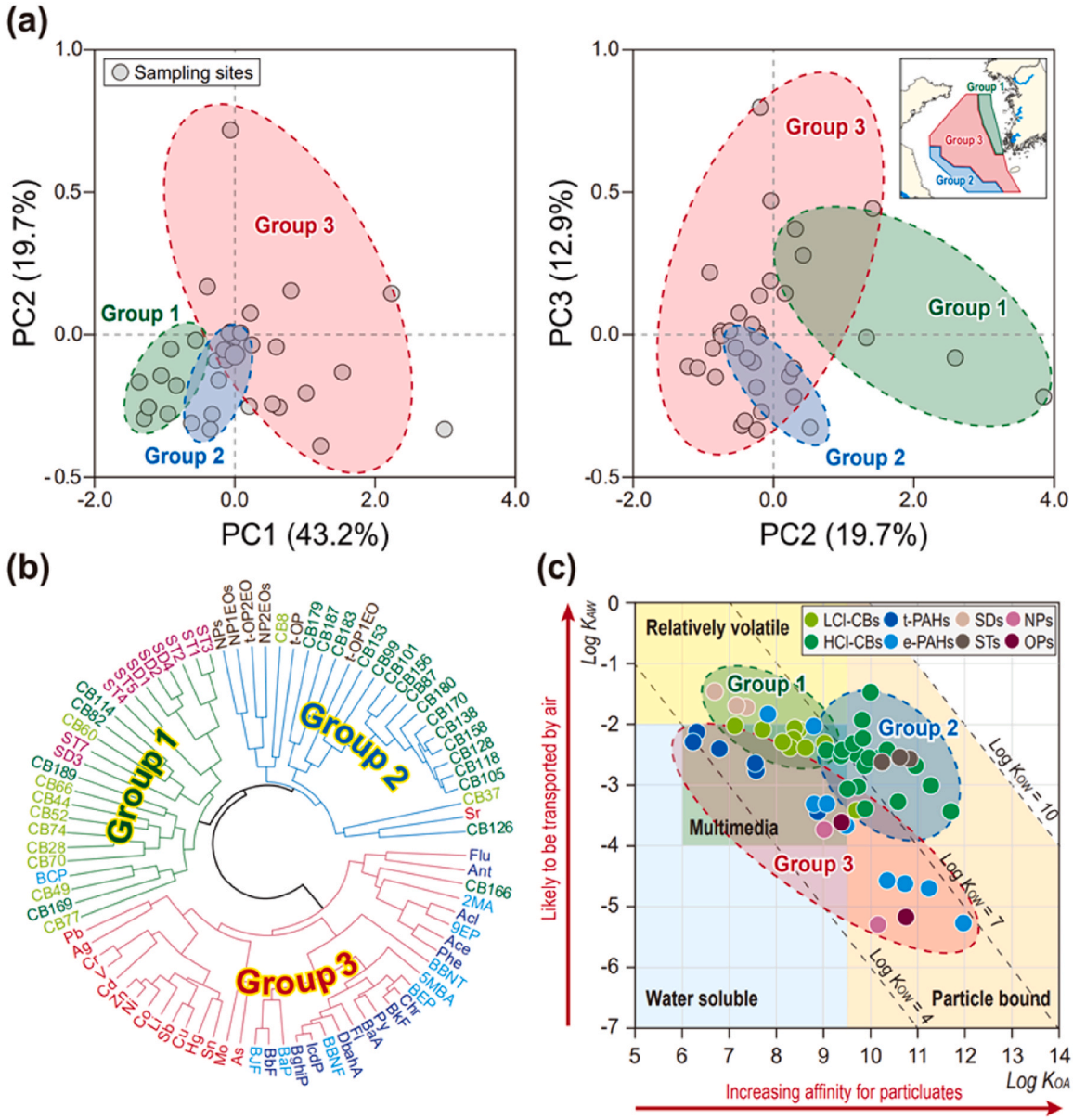

Fig. 6. **(a)** Result for principal component analysis based on PTSs and metals to identify regional differences. The Kaiser-Meyer-Olkin test was satisfied, with a result exceeding 0.5. **(b)** Result for cluster analysis to examine correlations between compounds (or elements) based on their spatial distributions. **(c)** Three groups were distinguished in the chemical space map utilizing the log K_{OA} (octanol-air partition coefficient), log K_{AW} (air-water partition coefficient), and log K_{OW} (octanol-water partition coefficient) of PTSs (LCl-CBs: di- to tetra-CBs; HCl-CBs: penta- to hepta-CBs).

significant negative correlation with sediment grain size (μm), indicating a grain size-dependent accumulation pattern. On the other hand, PCBs demonstrated a weak correlation with grain size and no significant correlation with OC contents. PCBs exhibited a distinct distribution pattern from other PTSs, showing weak or no correlation. The sources of PCBs were identified as combustion processes associated with industrial activities, such as iron and steel production [87]. Due to differences in physico-chemical properties, PCBs presented a different spatial distribution from other heavy metals and PTSs, suggesting a source-dependent accumulation pattern. PAHs showed a distribution pattern similar to that of heavy metals and were significantly correlated with OC contents and grain size. Spatially, the distributions of SOs and APs, which are highly accumulated near major rivers (Han River and Yangtze River), are thought to be mainly dependent on the amount of inflow [30,67].

PCA and cluster analysis were employed to discern similarities and differences among sampling sites within the study area and to identify compound- and element-specific behavior and accumulation patterns. As a result of PCA, the study area was distinguished into three groups (Fig. 6a). Group 1 mainly consisted of sampling sites near the west coast of South Korea, whereas Group 2 encompassed sites in the southwest of the Yellow Sea. Group 1 and Group 2 were primarily distinguished by PTSs and categorized as regions heavily influenced by PCBs, SOs, and APs. Group 3 was characterized by sites showing fine grain size, high OC content, and high concentrations of heavy metals and PAHs. These grouping results reflect the source, fate, and accumulation characteristics of PTSs and metals in the Yellow Sea environment, as highlighted by the spatial distribution and correlation analysis outcomes.

Cluster analysis was performed to identify target pollutants with similar behavior and accumulation characteristics and determine the controlling factors (Fig. 6b). The cluster analysis delineated three principal clusters. LCl-CBs and SOs were grouped, and these compounds mainly constituted Group 1. APs and HCl-CBs showed similar spatial distributions and were grouped together (Group 2). Compositional differences in PCBs between Group 1 and Group 2 were found. PCBs near the west coast of Korea were mainly LCl-CBs, while PCBs near the coast of China were predominantly HCl-CBs, showing regional differences. This appears to be because the composition of PCBs resulting from their origin differs between Korea and China. Meanwhile, t-PAHs, e-PAHs, and metals were classified into Group 3. They indicate that accumulation in the central Yellow Sea is influenced by sediment grain size and OC content rather than pollutant source and input route. Thus, it is difficult to determine their origin and contribution by country through concentration and composition, and it is necessary to apply additional pollutant identification tools, such as compound- and element-specific stable isotope ratios [88,89].

Interestingly, the accumulation patterns of PTSs varied for each group of compounds, such as PCBs, PAHs, SOs, and APs, and this phenomenon could be elucidated by partitioning coefficients, such as logarithm of log K_{OW} and log K_{OA} (Fig. 6c). Physical and chemical properties like partition coefficients can be utilized to characterize the behavior of compounds [90,91]. PTSs with relatively low log K_{OA} and log K_{OW} values (e.g., PAHs) tended to accumulate in the central Yellow Sea, while PTSs with relatively high logarithm of air-water partition coefficient (log K_{AW}) and log K_{OW} values tended to accumulate at sites near pollution sources. HCl-CBs and APs tend to associate with particulate matter due to their high log K_{OA}, while LCl-CBs and SDs exhibit behaviors with more dissolved phases, indicating a lower affinity for particulate association [92,93]. PAHs are slightly volatile and distributed through multiple environmental media. Due to these characteristics, they are believed to persist within the Yellow Sea and ultimately accumulate in its central regions. However, the distribution and accumulation of PTSs are not fully understood in terms of partitioning coefficients, and additional research is needed on the entire process of their inflow, behavior, and final accumulation in the future.

4. Conclusions

This study investigated the distribution, fate, and accumulation characteristics of PTSs and heavy metals in sediments across a wide area of the Yellow Sea. The central region of the Yellow Sea, referred to as CYSM, exhibited sedimentation of fine particles and elevated OC contents. Results of $\delta^{13}C$ revealed different origins of organic matter between the southern and central regions of the Yellow Sea. PTEs and PAHs showed relatively high concentrations in the central part of the Yellow Sea, suggesting their fate and accumulation corresponded with grain size and organic matter contents. Conversely, PCBs, SOs, and APs showed relatively higher concentrations around coastal areas, with distributions influenced by sources, distance, and physicochemical properties. Identifying potential sources of PTSs indicated that industrial products and combustion processes contribute to contaminating pollutants in the Yellow Sea. However, employing more robust and conservative source identification methods, such as compound- and/or element-specific isotope ratios, is essential for accurately evaluating sources of long-distance transported PTSs and metals. The findings of this study confirm the multifaceted factors influencing the fate and accumulation processes of PTSs and metals in offshore environments, providing evidence for the long-range transport and contribution to pollution of compounds sharing similar persistence and chemical properties.

Environmental implication

We investigated the accumulation characteristics of traditional pollutants, including PCBs, PAHs, and metals, and emerging toxicants, such as styrene oligomers and alkylphenols, in sediments of the Yellow Sea. The results showed compound- and elemental-specific accumulation patterns. PCBs, styrene oligomers, and alkylphenols showed a source-dependent distribution, whereas PAHs and metals were transported over long distances and accumulated in the central mud zone. The fate and accumulation of organic toxic substances were affected by their partition coefficients, such as log K_{OW} and log K_{OA}. These findings provide valuable insights into identifying the contributions of each country to pollution in the Yellow Sea.

CRediT authorship contribution statement

Youngnam Kim: Writing – original draft, Visualization, Investigation, Formal analysis, Data curation, Conceptualization. **Yeonjung Lee:** Writing – review & editing, Investigation, Formal analysis, Data curation. **Chang-Eon Lee:** Investigation, Formal analysis, Data curation. **Hyeryeong Jeong:** Investigation, Formal analysis, Data curation. **Kongtae Ra:** Writing – review & editing, Project administration, Investigation, Conceptualization. **Donghan Choi:** Project administration, Investigation, Funding acquisition. **Seongjin Hong:** Writing – review & editing, Writing – original draft, Supervision, Project administration, Investigation, Funding acquisition, Conceptualization.

Declaration of Competing Interest

The authors declare that they have no known competing financial interests or personal relationships that could have appeared to influence the work reported in this paper.

Data Availability

Data will be made available on request.

Acknowledgments

This research was supported by the Korea Institute of Marine Science & Technology Promotion (KIMST) funded by the Ministry of Oceans and

Fisheries (20210696, 20220534, and RS-2023-00256330). This work was also supported by the National Research Foundation of Korea (NRF) grant funded by the Korean government (MSIT) (No. 2022R1A4A1033825).

Appendix A. Supporting information

Supplementary data associated with this article can be found in the online version at doi:10.1016/j.jhazmat.2024.134926.

References

[1] Kaimoussi, A., Chafik, A., Mouzdahir, A., Bakkas, S., 2002. Diagnosis on the state of healthiness, quality of the coast and biological resources 'case of the Moroccan Atlantic coast'(City of El Jadida). C R Biol 325 (3), 253–260. https://doi.org/10.1016/S1631-0691(02)01424-5.

[2] Fang, T.-H., Hong, E., 1999. Mechanisms influencing the spatial distribution of trace metals in surficial sediments off the south-western Taiwan. Mar Pollut Bull 38 (11), 1026–1037. https://doi.org/10.1016/S0025-326X(99)00134-4.

[3] Sobek, A., Gustafsson, O., 2014. Deep water masses and sediments are main compartments for polychlorinated biphenyls in the Arctic Ocean. Environ Sci Technol 48 (12), 6719–6725. https://doi.org/10.1021/es500736q.

[4] Wolska, L., Mechlińska, A., Rogowska, J., Namieśnik, J., 2012. Sources and fate of PAHs and PCBs in the marine environment. Crit Rev Environ Sci Technol 42 (11), 1172–1189. https://doi.org/10.1080/10643389.2011.556546.

[5] Montuori, P., Aurino, S., Garzonio, F., Sarnacchiaro, P., Nardone, A., Triassi, M., 2016. Distribution, sources and ecological risk assessment of polycyclic aromatic hydrocarbons in water and sediments from Tiber River and estuary, Italy. Sci Total Environ 566, 1254–1267. https://doi.org/10.1016/j.scitotenv.2016.05.183.

[6] Webster, L., Russell, M., Walsham, P., Phillips, L.A., Hussy, I., Packer, G., Dalgarno, E.J., Moffat, C.F., 2011. An assessment of persistent organic pollutants in Scottish coastal and offshore marine environments. J Environ Monit 13 (5), 1288–1307. https://doi.org/10.1039/C1EM10100E.

[7] Tatarazako, N., Takao, Y., Kishi, K., Onikura, N., Arizono, K., Iguchi, T., 2002. Styrene dimers and trimers affect reproduction of daphnid (Ceriodaphnia dubia). Chemosphere 48 (6), 597–601. https://doi.org/10.1016/S0045-6535(02)00119-4.

[8] Galbán-Malagón, C., Berrojalbiz, N., Ojeda, M.-J., Dachs, J., 2012. The oceanic biological pump modulates the atmospheric transport of persistent organic pollutants to the Arctic. Nat Commun 3 (1), 862. https://doi.org/10.1038/ncomms1858.

[9] Ge, M., Wang, X., Yang, G., Wang, Z., Li, Z., Zhang, X., Xu, Q., 2021. Persistent organic pollutants (POPs) in deep-sea sediments of the tropical western Pacific Ocean. Chemosphere 277, 130267. https://doi.org/10.1016/j.chemosphere.2021.130267.

[10] Yang, S.Y., Jung, H.S., Lim, D.I., Li, C.X., 2003. A review on the provenance discrimination of sediments in the Yellow Sea. Earth-Sci Rev 63 (1-2), 93–120. https://doi.org/10.1016/S0012-8252(03)00033-3.

[11] Zhao, F., Wang, L., Elbadrawi, H., Shen, L.D., 1997. Temporal geographic information system and its application to transportation. Trans Res Rec 1593 (1), 47–54. https://doi.org/10.3141/1593-07.

[12] Hu, D., Li, Y., 1993. Study of ocean circulation. Mar Sci Study its Prospect China Qingdao Publ House 513–516.

[13] Yuan, H., Song, J., Li, X., Li, N., Duan, L., 2012. Distribution and contamination of heavy metals in surface sediments of the South Yellow Sea. Mar Pollut Bull 64 (10), 2151–2159. https://doi.org/10.1016/j.marpolbul.2012.07.040.

[14] Alexander, C., DeMaster, D., Nittrouer, C.A., 1991. Sediment accumulation in a modern epicontinental-shelf setting: the Yellow Sea. Mar Geol 98 (1), 51–72. https://doi.org/10.1016/0025-3227(91)90035-3.

[15] Fugate, D.C., Friedrichs, C.T., 2003. Controls on suspended aggregate size in partially mixed estuaries. Estuar Coast Shelf Sci 58 (2), 389–404. https://doi.org/10.1016/S0272-7714(03)00107-0.

[16] El-Shahawi, M., Hamza, A., Bashammakh, A.S., Al-Saggaf, W., 2010. An overview on the accumulation, distribution, transformations, toxicity and analytical methods for the monitoring of persistent organic pollutants. Talanta 80 (5), 1587–1597. https://doi.org/10.1016/j.talanta.2009.09.055.

[17] Peng, J.-f, Song, Y.-h, Yuan, P., Cui, X.-y, Qiu, G.-l, 2009. The remediation of heavy metals contaminated sediment. J Hazard Mater 161 (2-3), 633–640. https://doi.org/10.1016/j.jhazmat.2008.04.061.

[18] Hatje, V., Payne, T., Hill, D., McOrist, G., Birch, G., Szymczak, R., 2003. Kinetics of trace element uptake and release by particles in estuarine waters: effects of pH, salinity, and particle loading. Environ Int 29 (5), 619–629. https://doi.org/10.1016/S0160-4120(03)00049-7.

[19] Riba, I., Delvalls, T.Á., Forja, J.M., Gómez-Parra, A., 2004. The influence of pH and salinity on the toxicity of heavy metals in sediment to the estuarine clam Ruditapes philippinarum. Environ Toxicol Chem: Inter J 23 (5), 1100–1107. https://doi.org/10.1897/023-601.

[20] Hong, S., Lee, J., Lee, C., Yoon, S.J., Jeon, S., Kwon, B.-O., Lee, J.-H., Giesy, J.P., Khim, J.S., 2016. Are styrene oligomers in coastal sediments of an industrial area aryl hydrocarbon-receptor agonists? Environ Pollut 213, 913–921. https://doi.org/10.1016/j.envpol.2016.03.025.

[21] Ohyama, K.I., Nagai, F., Tsuchiya, Y., 2001. Certain styrene oligomers have proliferative activity on MCF-7 human breast tumor cells and binding affinity for human estrogen receptor. Environ Health Perspect 109 (7), 699–703. https://doi.org/10.1289/ehp.01109699.

[22] Renner, R., 1997. European bans on surfactant trigger transatlantic debate. Environ Sci Technol 31 (7), 316A–320A. https://doi.org/10.1021/es972366q.

[23] Klecka, G., Boethling, R., Franklin, J., Grady, L., Graham, D., Howard, P.H., Kannan, K., Larson, R., Mackay, D., Muir, D., 2000. Evaluation of persistance and long-range transport of organic chemicals in the environment. SETAC Pensacola, FL, USA.

[24] Roman, M., Van Dijk, L., Gutierrez, L., Vanoppen, M., Post, J., Wols, B., Cornelissen, E., Verliefde, A., 2019. Key physicochemical characteristics governing organic micropollutant adsorption and transport in ion-exchange membranes during reverse electrodialysis. Desalination 468, 114084. https://doi.org/10.1016/j.desal.2019.114084.

[25] Khalili, N.R., Scheff, P.A., Holsen, T.M., 1995. PAH source fingerprints for coke ovens, diesel and, gasoline engines, highway tunnels, and wood combustion emissions. Atmos Environ 29 (4), 533–542. https://doi.org/10.1016/1352-2310(94)00275-P.

[26] Yang, B., Zhou, L., Xue, N., Li, F., Li, Y., Vogt, R.D., Cong, X., Yan, Y., Liu, B., 2013. Source apportionment of polycyclic aromatic hydrocarbons in soils of Huanghuai Plain, China: Comparison of three receptor models. Sci Total Environ 443, 31–39. https://doi.org/10.1016/j.scitotenv.2012.10.094.

[27] Harrison, R.M., Smith, D., Luhana, L., 1996. Source apportionment of atmospheric polycyclic aromatic hydrocarbons collected from an urban location in Birmingham, UK. Environ. Sci. Technol. 30 (3), 825–832. https://doi.org/10.1021/es950252d.

[28] Bouloubassi, I., Saliot, A., 1993. Dissolved, particulate and sedimentary naturally derived polycyclic aromatic hydrocarbons in a coastal environment: geochemical significance. Mar Chem 42 (2), 127–143. https://doi.org/10.1016/0304-4203(93)90242-G.

[29] Ra, K., Kim, J.-K., Hong, S.H., Yim, U.H., Shim, W.J., Lee, S.-Y., Kim, Y.-O., Lim, J., Kim, E.-S., Kim, K.-T., 2014. Assessment of pollution and ecological risk of heavy metals in the surface sediments of Ulsan Bay, Korea. Ocean Sci J 49 (3), 279–289. https://doi.org/10.1007/s12601-014-0028-3.

[30] Kim, Y., Hong, S., Lee, J., Yoon, S.J., An, Y., Kim, M.-S., Jeong, H.-D., Khim, J.S., 2021. Spatial distribution and source identification of traditional and emerging persistent toxic substances in the offshore sediment of South Korea. Sci Total Environ 789, 147996. https://doi.org/10.1016/j.scitotenv.2021.147996.

[31] Lee, J., Kim, Y., Cha, J., Kim, D., Jang, K., Kim, J.-H., Nam, S.-I., Hong, S., 2023. Distributions and potential sources of polychlorinated biphenyls and polycyclic aromatic hydrocarbons in the glacimarine sediments of Arctic Svalbard. Mar Pollut Bull 189, 114740. https://doi.org/10.1016/j.marpolbul.2023.114740.

[32] Hopke, P.K., 2003. Recent developments in receptor modeling. J Chemom 17 (5), 255–265. https://doi.org/10.1002/cem.796.

[33] Qishlaqi, A., Beiramali, F., 2019. Potential sources and health risk assessment of polycyclic aromatic hydrocarbons in street dusts of Karaj urban area, northern Iran. J Environ Health Sci 17, 1029–1044. https://doi.org/10.1007/s40201-019-00417-3.

[34] Adamo, P., Arienzo, M., Imperato, M., Naimo, D., Nardi, G., Stanzione, D., 2005. Distribution and partition of heavy metals in surface and sub-surface sediments of Naples city port. Chemosphere 61 (6), 800–809. https://doi.org/10.1016/j.chemosphere.2005.04.001.

[35] Zhao, Y.-Y., Jiang, R.-H., Yan, M.-C., 1995. Abundance of chemical elements in continental shelf sediment of China. Geo-Mar Lett 15, 71–76. https://doi.org/10.1007/BF01275409.

[36] Zhang, J., Liu, C., 2002. Riverine composition and estuarine geochemistry of particulate metals in China–weathering features, anthropogenic impact and chemical fluxes. Estuar Coast Shelf Sci 54 (6), 1051–1070. https://doi.org/10.1006/ecss.2001.0879.

[37] Lee, H., Jeong, K., Han, S., Bahk, K., 1988. Heavy minerals indicative of Holocene transgression in the southeastern Yellow Sea. Cont Shelf Res 8 (3), 255–266. https://doi.org/10.1016/0278-4343(88)90032-5.

[38] Hong, G., Zhang, J., Kim, S., Chung, C., Yang, S., 2002. East Asian marginal seas: river-dominated ocean margin. Impact of Interface Exchange on the Biogeochemical Processes of the Yellow and East China Seas, edited by: Hong, GH, Zhang, J., and Chung, CS, Bum Shin Press, Seoul, 233–260.

[39] Park, S.-C., Lee, H.-H., Han, H.-S., Lee, G.-H., Kim, D.-C., Yoo, D.-G., 2000. Evolution of late Quaternary mud deposits and recent sediment budget in the southeastern Yellow Sea. Mar. Geol. 170 (3–4), 271–288. https://doi.org/10.1016/S0025-3227(00)00099-2.

[40] Li, C.X., Zhang, J.Q., Deng, B., 2001. Holocene regression and the tidal radial sand ridge system formation in the Jiangsu coastal zone, east China. Mar. Geol. 173 (1–4), 97–120. https://doi.org/10.1016/S0025-3227(00)00169-9.

[41] Hu, L., Guo, Z., Feng, J., Yang, Z., Fang, M., 2009. Distributions and sources of bulk organic matter and aliphatic hydrocarbons in surface sediments of the Bohai Sea, China. Mar Chem 113 (3-4), 197–211. https://doi.org/10.1016/j.marchem.2009.02.001.

[42] Kao, S.J., Lin, F.J., Liu, K.K., 2003. Organic carbon and nitrogen contents and their isotopic compositions in surficial sediments from the East China Sea shelf and the southern Okinawa Trough. Deep Res Ii 50 (6), 1203–1217. https://doi.org/10.1016/S0967-0645(03)00018-3.

[43] Park, Y., Khim, B., 1992. Origin and dispersal of recent clay minerals in the Yellow Sea. Mar. Geol. 104 (1–4), 205–213. https://doi.org/10.1016/0025-3227(92)90095-Y.

[44] Schubert, C.J., Calvert, S.E., 2001. Nitrogen and carbon isotopic composition of marine and terrestrial organic matter in Arctic Ocean sediments:: implications for nutrient utilization and organic matter composition. Deep Res PT I 48 (3), 789–810. https://doi.org/10.1016/S0967-0637(00)00069-8.

[45] Liu, X., Tang, D., Ge, C., 2020. Distribution and sources of organic carbon, nitrogen and their isotopic composition in surface sediments from the southern Yellow Sea, China. Mar Pollut Bull 150, 110716. https://doi.org/10.1016/j.marpolbul.2019.110716.
[46] Pataki, D.E., Bowling, D.R., Ehleringer, J.R., 2003. Seasonal cycle of carbon dioxide and its isotopic composition in an urban atmosphere: Anthropogenic and biogenic effects. J Geophys Res 108 (D23). https://doi.org/10.1029/2003JD003865.
[47] Rau, G., Takahashi, T., Des Marais, D., Repeta, D., Martin, J., 1992. The relationship between δ13C of organic matter and [CO_2 (aq)] in ocean surface water: data from a JGOFS site in the northeast Atlantic Ocean and a model. Geochim Cosmochim Acta 56 (3), 1413–1419. https://doi.org/10.1016/0016-7037(92)90073-R.
[48] Tesán-Onrubia, J.A., Tedetti, M., Carlotti, F., Tenaille, M., Guilloux, L., Pagano, M., Lebreton, B., Guillou, G., Fierro-González, P., Guigue, C., 2023. Spatial variations of biochemical content and stable isotope ratios of size-fractionated plankton in the Mediterranean Sea (MERITE-HIPPOCAMPE campaign). Mar Pollut Bull 189, 114787. https://doi.org/10.1016/j.marpolbul.2023.114787.
[49] Lee, Y., Choi, D.H., Lee, H., Hyun, M.J., Kim, G., Lee, H., Yang, W., Kim, J., Won, J., Ra, K., Jeong, H., Choi, J.Y., Lee, S., Kim, M., Noh, J.-H., 2022. Changes in the characteristics of organic matter associated with hydrodynamics and phytoplankton size structure in the central-eastern Yellow Sea. Sci. Total Environ. 807, 151781. https://doi.org/10.1016/j.scitotenv.2021.151781.
[50] Tang, D., Liu, X., Zou, X., 2018. An improved method for integrated ecosystem health assessments based on the structure and function of coastal ecosystems: A case study of the Jiangsu coastal area, China. Ecol Indic 84, 82–95. https://doi.org/10.1016/j.ecolind.2017.08.031.
[51] Huang, Y.-J., Lee, C.-L., Fang, M.-D., 2011. Distribution and source differentiation of PAHs and PCBs among size and density fractions in contaminated harbor sediment particles and their implications in toxicological assessment. Mar. Pollut. Bull. 62 (2), 432–439. https://doi.org/10.1016/j.marpolbul.2010.11.022.
[52] Ikonomou, M., Sather, P., Oh, J.-E., Choi, W.-Y., Chang, Y.-S., 2002. PCB levels and congener patterns from Korean municipal waste incinerator stack emissions. Chemosphere 49 (2), 205–216. https://doi.org/10.1016/S0045-6535(02)00102-9.
[53] Yang, H., Zhuo, S., Xue, B., Zhang, C., Liu, W., 2012. Distribution, historical trends and inventories of polychlorinated biphenyls in sediments from Yangtze River Estuary and adjacent East China Sea. Environ Pollut 169, 20–26. https://doi.org/10.1016/j.envpol.2012.05.003.
[54] Pedersen, K.B., Lejon, T., Jensen, P.E., Ottosen, L.M., 2015. Chemometric analysis for pollution source assessment of harbour sediments in Arctic locations. Water, Air, Soil Pollut 226 (5), 150. https://doi.org/10.1007/s11270-015-2416-4.
[55] Hong, S., Kim, Y., Lee, Y., Yoon, S.J., Lee, C., Liu, P., Kwon, B.-O., Hu, W., Khim, J. S., 2022. Distributions and potential sources of traditional and emerging polycyclic aromatic hydrocarbons in sediments from the lower reach of the Yangtze River, China. Sci Total Environ 815, 152831. https://doi.org/10.1016/j.scitotenv.2021.152831.
[56] Choi, H.G., Moon, H.B., Choi, M., Yu, J., 2011. Monitoring of organic contaminants in sediments from the Korean coast: Spatial distribution and temporal trends (2001–2007). Mar Pollut Bull 62 (6), 1352–1361. https://doi.org/10.1016/j.marpolbul.2011.03.029.
[57] Liu, J.P., Li, A.C., Xu, K.H., Velozzi, D.M., Yang, Z.S., Milliman, J.D., DeMaster, D. J., 2006. Sedimentary features of the Yangtze River-derived along-shelf clinoform deposit in the East China Sea. Cont Shelf Res 26 (17), 2141–2156. https://doi.org/10.1016/j.csr.2006.07.013.
[58] Lin, T., Hu, L., Guo, Z., Qin, Y., Yang, Z., Zhang, G., Zheng, M., 2011. Sources of polycyclic aromatic hydrocarbons to sediments of the Bohai and Yellow Seas in East Asia. J Geophys Res 116 (D23). https://doi.org/10.1029/2011JD015722.
[59] Zhang, Y., Schauer, J.J., Zhang, Y., Zeng, L., Wei, Y., Liu, Y., Shao, M., 2008. Characteristics of particulate carbon emissions from real-world Chinese coal combustion. Environ Sci Technol 42 (14), 5068–5073. https://doi.org/10.1021/es7022576.
[60] Gao, B., Guo, H., Wang, X.-M., Zhao, X.-Y., Ling, Z.-H., Zhang, Z., Liu, T.-Y., 2013. Tracer-based source apportionment of polycyclic aromatic hydrocarbons in PM 2.5 in Guangzhou, southern China, using positive matrix factorization (PMF). Environ Sci Pollut Res 20 (4), 2398–2409. https://doi.org/10.1007/s11356-012-1129-0.
[61] Kavouras, I.G., Koutrakis, P., Tsapakis, M., Lagoudaki, E., Stephanou, E.G., Von Baer, D., Oyola, P., 2001. Source apportionment of urban particulate aliphatic and polynuclear aromatic hydrocarbons (PAHs) using multivariate methods. Environ Sci Technol 35 (11), 2288–2294. https://doi.org/10.1021/es001540z.
[62] Bosch, C., Andersson, A., Kruså, M., Bandh, C., Hovorková, I., Klánová, J., Knowles, T.D.J., Pancost, R.D., Evershed, R.P., Gustafsson, Ö., 2015. Source Apportionment of Polycyclic Aromatic Hydrocarbons in Central European Soils with Compound-Specific Triple Isotopes (δ13C, Δ14C, and δ2H). Environ Sci Technol 49 (13), 7657–7665. https://doi.org/10.1021/acs.est.5b01190.
[63] Kim, Y., Hong, S., Jun, L., Lee, Y., Kim, M., Yim, U.H., Khim, J.S., Shin, K.H., 2023. Use of molecular composition and compound-specific isotope analysis for source appointment of PAHs in sediments of a highly industrialized area. Environ Pollut 337, 122546. https://doi.org/10.1016/j.envpol.2023.122546.
[64] Kwon, B.G., Koizumi, K., Chung, S.-Y., Kodera, Y., Kim, J.-O., Saido, K., 2015. Global styrene oligomers monitoring as new chemical contamination from polystyrene plastic marine pollution. J Hazard Mater 300, 359–367. https://doi.org/10.1016/j.jhazmat.2015.07.039.
[65] Tian, Z., Kim, S.-K., Hyun, J.-H., 2020. Environmental distribution of styrene oligomers (SOs) coupled with their source characteristics: Tracing the origin of SOs in the environment. J Hazard Mater 398, 122968. https://doi.org/10.1016/j.jhazmat.2020.122968.
[66] Soares, A., Guieysse, B., Jefferson, B., Cartmell, E., Lester, J., 2008. Nonylphenol in the environment: a critical review on occurrence, fate, toxicity and treatment in wastewaters. Environ Int 34 (7), 1033–1049. https://doi.org/10.1016/j.envint.2008.01.004.
[67] Zhao, J.-L., Huang, Z., Zhang, Q.-Q., Ying-He, L., Wang, T.-T., Yang, Y.-Y., Ying, G.-G., 2021. Distribution and mass loads of xenoestrogens bisphenol a, 4-nonylphenol, and 4-tert-octylphenol in rainfall runoff from highly urbanized regions: A comparison with point sources of wastewater. J Hazard Mater 401, 123747. https://doi.org/10.1016/j.jhazmat.2020.123747.
[68] Gao, S., Wang, Y.P., 2008. Changes in material fluxes from the Changjiang River and their implications on the adjoining continental shelf ecosystem. Cont Shelf Res 28 (12), 1490–1500. https://doi.org/10.1016/j.csr.2007.02.010.
[69] Liu, M., Chen, J., Sun, X., Hu, Z., Fan, D., 2019. Accumulation and transformation of heavy metals in surface sediments from the Yangtze River estuary to the East China Sea shelf. Environ Pollut 245, 111–121. https://doi.org/10.1016/j.envpol.2018.10.128.
[70] Wang, C., Zou, X., Gao, J., Zhao, Y., Yu, W., Li, Y., Song, Q., 2016. Pollution status of polycyclic aromatic hydrocarbons in surface sediments from the Yangtze River Estuary and its adjacent coastal zone. Chemosphere 162, 80–90. https://doi.org/10.1016/j.chemosphere.2016.07.075.
[71] An, Y., Hong, S., Yoon, S.J., Cha, J., Shin, K.-H., Khim, J.S., 2020. Current contamination status of traditional and emerging persistent toxic substances in the sediments of Ulsan Bay, South Korea. Mar Pollut Bull 160, 111560. https://doi.org/10.1016/j.marpolbul.2020.111560.
[72] Isobe, T., Nishiyama, H., Nakashima, A., Takada, H., 2001. Distribution and behavior of nonylphenol, octylphenol, and nonylphenol monoethoxylate in Tokyo Metropolitan Area: Their association with aquatic particles and sedimentary distributions. Environ Sci Technol 35 (6), 1041–1049. https://doi.org/10.1021/es001250i.
[73] Maguire, R.J., 1999. Review of the persistence of nonylphenol and nonylphenol ethoxylates in aquatic environments. Water Quality Research Journal 34 (1), 37–78. https://doi.org/10.2166/wqrj.1999.003.
[74] Lyubas, A.A., Kuznetsova, I.A., Bovykina, G.V., Eliseeva, T.A., Gofarov, M.Y., Khrebtova, I.S., Kondakov, A.V., Malkov, A.V., Mavromatis, V., Shevchenko, A.R., 2023. Trace element patterns in shells of mussels (bivalvia) allow to distinguish between fresh-and brackish-water coastal environments of the subarctic and boreal zone. Water 15 (20), 3625. https://doi.org/10.3390/w15203625.
[75] El Bilali, L., Rasmussen, P., Hall, G., Fortin, D., 2002. Role of sediment composition in trace metal distribution in lake sediments. Appl Geochem 17 (9), 1171–1181. https://doi.org/10.1016/S0883-2927(01)00132-9.
[76] Bown, J., Laan, P., Ossebaar, S., Bakker, K., Rozema, P., de Baar, H.J., 2017. Bioactive trace metal time series during Austral summer in Ryder Bay, Western Antarctic Peninsula. Deep Res Ii 139, 103–119. https://doi.org/10.1016/j.dsr2.2016.07.004.
[77] Laes, A., Blain, S., Laan, P., Ussher, S., Achterberg, E.P., Tréguer, P., De Baar, H., 2007. Sources and transport of dissolved iron and manganese along the continental margin of the Bay of Biscay. Biogeosciences 4 (2), 181–194. https://doi.org/10.5194/bg-4-181-2007.
[78] Smrzka, D., Zwicker, J., Bach, W., Feng, D., Himmler, T., Chen, D., Peckmann, J., 2019. The behavior of trace elements in seawater, sedimentary pore water, and their incorporation into carbonate minerals: a review. Facies 65, 1–47. https://doi.org/10.1007/s10347-019-0581-4.
[79] Soto-Jiménez, M., Páez-Osuna, F., Ruiz-Fernández, A., 2003. Geochemical evidences of the anthropogenic alteration of trace metal composition of the sediments of Chiricahueto marsh (SE Gulf of California). Environ Pollut 125 (3), 423–432. https://doi.org/10.1016/S0269-7491(03)00083-6.
[80] Rosenheim, B.E., Swart, P.K., Thorrold, S.R., Willenz, P., Berry, L., Latkoczy, C., 2004. High-resolution Sr/Ca records in sclerosponges calibrated to temperature in situ. Geology 32 (2), 145–148. https://doi.org/10.1130/g20117.1.
[81] Yang, S., Lim, D., Jung, H., Oh, B., 2004. Geochemical composition and provenance discrimination of coastal sediments around Cheju Island in the southeastern Yellow Sea. Mar Geol 206 (1-4), 41–53. https://doi.org/10.1016/j.margeo.2004.01.005.
[82] Chung, C.-S., Song, K.-H., Choi, K.-Y., Kim, Y.-I., Kim, H.-E., Jung, J.-M., Kim, C.-J., 2017. Variations in the concentrations of heavy metals through enforcement of a rest-year system and dredged sediment capping at the Yellow Sea-Byung dumping site, Korea. Mar Pollut Bull 124 (1), 512–520. https://doi.org/10.1016/j.marpolbul.2017.07.032.
[83] Liu, Q., Yang, P., Hu, Z., Shu, Q., Chen, Y., 2022. Identification of the sources and influencing factors of the spatial variation of heavy metals in surface sediments along the northern Jiangsu coast. Ecol Indic 137, 108716. https://doi.org/10.1016/j.ecolind.2022.108716.
[84] Martin, J., Lusher, A., Thompson, R.C., Morley, A., 2017. The Deposition and accumulation of microplastics in marine sediments and bottom water from the Irish Continental Shelf. Sci Rep 7 (1), 10772. https://doi.org/10.1038/s41598-017-11079-2.
[85] Bergamaschi, B.A., Tsamakis, E., Keil, R.G., Eglinton, T.I., Montluçon, D.B., Hedges, J.I., 1997. The effect of grain size and surface area on organic matter, lignin and carbohydrate concentration, and molecular compositions in Peru Margin sediments. Geochim Cosmochim Acta 61 (6), 1247–1260. https://doi.org/10.1016/S0016-7037(96)00394-8.
[86] Tansel, B., Rafiuddin, S., 2016. Heavy metal content in relation to particle size and organic content of surficial sediments in Miami River and transport potential. Int J Sediment Res 31 (4), 324–329. https://doi.org/10.1016/j.ijsrc.2016.05.004.
[87] Aydin, Y.M., Kara, M., Dumanoglu, Y., Odabasi, M., Elbir, T., 2014. Source apportionment of polycyclic aromatic hydrocarbons (PAHs) and polychlorinated

biphenyls (PCBs) in ambient air of an industrial region in Turkey. Atmos Environ 97, 271–285. https://doi.org/10.1016/j.atmosenv.2014.08.032.
[88] Glibert, P.M., Middelburg, J.J., McClelland, J.W., Jake Vander Zanden, M., 2019. Stable isotope tracers: Enriching our perspectives and questions on sources, fates, rates, and pathways of major elements in aquatic systems. Limnol Oceanogr 64 (3), 950–981. https://doi.org/10.1002/lno.11087.
[89] Tanimizu, M., Sohrin, Y., Hirata, T., 2013. Heavy element stable isotope ratios: analytical approaches and applications. Anal Bioanal Chem 405 (9), 2771–2783. https://doi.org/10.1007/s00216-013-6728-1.
[90] Moeckel, C., Monteith, D.T., Llewellyn, N.R., Henrys, P.A., Pereira, M.G., 2014. Relationship between the Concentrations of Dissolved Organic Matter and Polycyclic Aromatic Hydrocarbons in a Typical U.K. Upland Stream. Environ Sci Technol 48 (1), 130–138. https://doi.org/10.1021/es403707q.
[91] Wang, W., Qu, X., Lin, D., Yang, K., 2021. Octanol-water partition coefficient (logKow) dependent movement and time lagging of polycyclic aromatic hydrocarbons (PAHs) from emission sources to lake sediments: A case study of Taihu Lake, China. Environ Pollut 288, 117709. https://doi.org/10.1016/j.envpol.2021.117709.
[92] Mitra, S., Dickhut, R.M., 1999. Three-phase modeling of polycyclic aromatic hydrocarbon association with pore-water-dissolved organic carbon. Environ Toxicol Chem 18 (6), 1144–1148. https://doi.org/10.1002/etc.5620180611.
[93] Thibodeaux, L.J., Valsaraj, K.T., Reible, D.D., 1993. Associations between polychlorinated biphenyls and suspended solids in natural waters: An evaluation of the uptake rate by particles. Water Sci Technol 28 (8-9), 215–221. https://doi.org/10.2166/wst.1993.0621.

<Journal of Hazardous Materials>

Supplementary materials for

Compound- and element-specific accumulation characteristics of persistent toxic substances and metals in sediments of the Yellow Sea

Youngnam Kim, Yeonjung Lee, Chang-Eon Lee, Hyeryeong Jeong, Kongtae Ra,

Donghan Choi, Seongjin Hong*

This PDF file includes:

Number of pages: 18

Number of Supplementary Tables: 10, Tables S1 to S10

Number of Supplementary Figures: 4, Figs. S1 to S4

References

***Corresponding author.**

Department of Marine Environmental Sciences, Chungnam National University

99 Daehak-ro, Yuseong-gu, Daejeon 34134, Republic of Korea.

Tel.: +82 42 821 6436; fax: +82 42 822 8173. *E-mail*: hongseongjin@cnu.ac.kr (S. Hong).

Supplementary Tables

Table S1. Locations of sampling sites and summary of grain size, total organic carbon (OC) contents, total nitrogen (TN) contents, and stable isotope ratios ($\delta^{13}C$ and $\delta^{15}N$) in sediments of the Yellow Sea.

Latitude (N°)	Longitude (E°)	Sites	Depth (m)	Mean grain size (μm)	(Ø)	Sand (%)	Silt (%)	Clay (%)	OC (%)	TN (%)	$\delta^{13}C$ (‰)	$\delta^{15}N$ (‰)
32.2	126.5	N3201	103	10	6.6	7.7	84	8.2	0.62	0.11	–21.05	4.66
	126.0	N3203	89	9.1	6.8	15	74	11	0.49	0.10	–21.09	5.42
	125.5	N3205	73	7.1	7.1	4.2	81	15	0.63	0.13	–21.04	5.58
	125.0	N3207	55	15	6.1	24	70	5.2	0.45	0.08	–21.07	5.46
	124.5	N3209	42	23	5.5	37	58	5.4	0.39	0.06	–20.94	4.76
	124.0	N3211	41	120	3.0	53	44	3.7	0.27	0.04	–20.73	5.13
33	126.0	N3301	105	170	2.5	54	42	4.1	0.22	0.05	–21.19	5.32
	125.0	N3305	80	10	6.6	18	73	9.6	0.53	0.09	–21.20	5.36
	124.5	N3307	66	16	6.0	31	64	5.5	0.34	0.07	–21.25	5.48
	124.0	N3309	50	23	5.5	37	58	5.3	0.38	0.06	–21.06	5.21
	123.5	N3311	35	18	5.8	32	64	4.6	0.40	0.07	–21.08	5.38
	123.1	N3313	35	30	5.1	41	55	4.7	0.30	0.05	–21.13	4.69
34	126.0	N3401	80	20	5.6	35	60	5.7	0.27	0.05	–21.47	5.40
	125.5	N3404	70	17	5.9	21	72	6.8	0.33	0.06	–21.65	5.90
	125.0	N3407	95	33	4.9	46	49	4.6	0.26	0.05	–21.55	5.75
	124.0	N3411	80	14	6.2	18	75	7.8	0.57	0.10	–21.53	5.45
	123.5	N3413	70	11	6.4	17	73	9.8	0.47	0.09	–21.54	5.55
	123.0	N3415	70	11	6.6	6.8	83	11	0.53	0.09	–21.76	5.13
	122.5	N3417	40	40	4.7	29	68	3.3	0.25	0.05	–22.08	4.30
	122.0	N3419	18	88	3.5	69	30	1.3	0.12	0.02	–21.19	3.87
35	125.7	N3503	31	20	5.7	6.2	88	5.7	0.48	0.08	–21.60	5.70
	125.0	N3507	90	120	3.0	60	38	2.3	0.27	0.04	–22.27	5.68
	124.5	N3509	90	25	5.3	30	65	5.0	0.49	0.09	–21.88	5.69
	124.0	N3511	80	20	5.7	20	74	6.3	0.54	0.10	–21.92	5.40
	123.5	N3513	77	13	6.3	4.1	87	9.3	0.80	0.13	–21.96	5.72
	123.0	N3515	72	12	6.4	2.2	88	9.7	0.80	0.14	–21.96	5.53
	122.5	N3517	66	14	6.2	3.4	88	8.1	0.78	0.13	–21.93	5.36
	122.0	N3519	50	29	5.1	25	70	4.7	0.45	0.08	–21.96	5.06
36	125.3	N3605	75	290	1.8	94	6.1	0.10	0.10	0.02	–22.00	5.42
	124.6	N3608	87	88	3.5	61	37	1.8	0.55	0.10	–22.31	5.15
	124.0	N3611	77	15	6.0	6.8	85	8.0	1.1	0.18	–21.97	5.54
	123.0	N3615	70	15	6.0	3.5	88	8.1	1.0	0.18	–21.73	5.56
37	125.0	N3706	47	240	2.0	100	0.0	0.0	0.11	0.02	–21.08	5.75
	124.5	N3709	78	190	2.4	93	7.2	0.12	0.10	0.04	–21.84	4.96
	124.0	N3711	79	93	3.4	65	32	2.3	0.26	0.05	–22.16	5.37

Table S2. Target compounds, abbreviations, and target ions in the instrumental analysis, as well as method detection limits and recoveries of surrogate standards.

Target compounds	Abbreviations	Quantification ion	Confirmation ion	Method detection limit (ng g^{-1} dw)
Polychlorinated biphenlys (PCBs)				
2,4'-Dichlorobiphenyl	CB8	222	224	0.03
2,4,4'-Trichlorobiphenyl	CB28	256	258	0.03
2,2',5,5'-Tetrachlorobiphenyl	CB52	292	290	0.02
2,2',4,5'-Tetrachlorobiphenyl	CB49	292	290	0.02
2,2',3,5'-Tetrachlorobiphenyl	CB44	292	290	0.03
3,4,4'-Trichlorobiphenyl	CB37	256	258	0.02
2,4,4',5-Tetrachlorobiphenyl	CB74	292	290	0.02
2,3',4',5-Tetrachlorobiphenyl	CB70	292	290	0.01
2,3',4,4'-Tetrachlorobiphenyl	CB66	292	290	0.03
2,3,4,4'-Tetrachlorobiphenyl	CB60	292	290	0.03
2,2',4,5,5'-Pentachlorobiphenyl	CB101	326	324	0.02
2,2',4,4',5-Pentachlorobiphenyl	CB99	326	328	0.02
2,2',3,4,5'-Pentachlorobiphenyl	CB87	292	290	0.02
3,3',4,4'-Tetrachlorobiphenyl	CB77	326	256	0.01
2,2',3,3',4-Pentachlorobiphenyl	CB82	338	340	0.03
2,3',4,4',5-Pentachlorobiphenyl	CB118	326	328	0.03
2,3,4,4',5-Pentachlorobiphenyl	CB114	326	328	0.02
2,2',4,4',5,5'-Hexachlorobiphenyl	CB153	360	362	0.02
2,3,3',4,4'-Pentachlorobiphenyl	CB105	326	324	0.02
2,2',3,3',5,6,6'-Heptachlorobiphenyl	CB179	396	398	0.03
2,2',3,4,4',5'-Hexachlorobiphenyl	CB138	360	362	0.02
2,3,3',4,4',6-Hexachlorobiphenyl	CB158	326	328	0.03
3,3',4,4',5-Pentachlorobiphenyl	CB126	360	362	0.02
2,3,4,4',5,6-Hexachlorobiphenyl	CB166	394	396	0.02
2,2',3,4',5,5',6-Heptachlorobiphenyl	CB187	394	396	0.02
2,2',3,4,4',5',6-Heptachlorobiphenyl	CB183	360	362	0.02
2,2',3,3',4,4'-Hexachlorobiphenyl	CB128	440	442	0.02
2,3,3',4,4',5-Hexachlorobiphenyl	CB156	360	362	0.02
2,2',3,4,4',5,5'-Heptachlorobiphenyl	CB180	394	396	0.03
3,3',4,4',5,5'-Hexachlorobiphenyl	CB169	360	362	0.03
2,2',3,3',4,4',5-Heptachlorobiphenyl	CB170	394	396	0.03
2,3,3',4,4',5,5'-Heptachlorobiphenyl	CB189	476	478	0.03
Traditional Polycyclic aromatic hydrocarbons (t-PAHs)				
Acenaphthylene	Acl	152	151	3.51
Acenaphthene	Ace	153	154	4.23
Fluorene	Flu	166	165	4.41
Phenanthrene	Phe	178	176	4.38
Anthracene	Ant	178	176	5.27
Fluoranthene	Fl	202	200	3.37
Pyrene	Py	202	200	2.83
Benzo[*a*]anthracene	BaA	228	226	2.11
Chrysene	Chr	228	226	2.59
Benzo[*b*]fluoranthene	BbF	252	253	1.82
Benzo[*k*]fluoranthene	BkF	252	253	0.55
Benzo[*a*]pyrene	BaP	252	253	2.76
Indeno[*1,2,3-cd*]pyrene	IcdP	276	138	4.04
Dibenz[*a,h*]anthracene	DbahA	278	276	3.73
Benzo[*g,h,i*]perylene	BghiP	276	138	5.41
Emerging PAHs (e-PAHs)				

Benzo[*b*]naphtho[*2,3-d*]furan	BBNF	218	189	2.36
Benzo[*b*]naphtho[*2,1-d*]thiophene	BBNT	234	235	1.11
5-Methylbenzo[*a*]anthracene	5MBA	242	241	1.35
4,5-Methanochrysene	4,5MC	239	240	3.10
1-Methylchrysene	1MC	242	241	1.45
7-Methylbenz[a]anthracene	7MbA	242	241	1.98
7,12-Dimethylbenz[a]anthracene	7,12DbA	256	241	1.07
10-Methylbenzo[a]pyrene	10MbA	266	256	2.83
Styrene oligomers (SOs)				
1,3-Diphenylpropane	SD1	105	196	0.19
cis-1,2-Diphenylcyclobutane	SD2	78	208	0.19
2,4-Diphenyl-1-butene	SD3	104	208	0.89
trans-1,2-Diphenylcyclobutane	SD4	78	208	0.11
2,4,6-Triphenyl-1-hexene	ST1	117	194	0.63
1e-Phenyl-4e-(1-phenylethyl)-tetralin	ST2	129	207	0.66
1a-Phenyl-4e-(1-phenylethyl)-tetralin	ST3	129	207	0.31
1a-Phenyl-4a-(1-phenylethyl)-tetralin	ST4	129	207	0.70
1e-Phenyl-4a-(1-phenylethyl)-tetralin	ST5	207	105	0.41
1,3,5-Triphenylcyclohexane	ST6	117	104	0.88
Alkylphenols (APs)				
4-*tert*-Octylphenol	t-OP	207	221	0.12
4-*tert*-Octylphenol monoethoxylate	t-OP1EO	251	265	0.61
4-*tert*-Octylphenol diethoxylate	t-OP2EO	295	309	0.08
Nonylphenols	NPs	207	221	3.7
Nonylphenol monoethoxylates	NP1EOs	251	265	0.45
Nonylphenol diethoxylates	NP2EOs	295	309	1.5
Internal standard				
2-Fluorobiphenyl	IS	172	171	

Surrogate standards		**Quantification ion**	**Confirmation ion**	**Surrogate recovery (%, mean ± SD)**
Polychlorinated biphenyl (PCBs)				
^{13}C-labeled CB 28		268	270	106 ± 7
^{13}C-labeled CB 52		304	302	99 ± 6
^{13}C-labeled CB 101		326	328	102 ± 6
^{13}C-labeled CB 153		372	374	109 ± 7
^{13}C-labeled CB 138		360	362	110 ± 6
^{13}C-labeled CB 180		406	408	114 ± 7
^{13}C-labeled CB 209		510	512	115 ± 8
Polycyclic aromatic hydrocarbons (PAHs)				
Acenaphthene-d10	Ace-d10	164	162	87 ± 11
Phenanthrene-d10	Phe-d10	188	189	74 ± 13
Chrysene-d12	Chr-d12	240	236	88 ± 11
Perylene-d12	Pery-d12	264	270	90 ± 12
Alkylphenols (APs)				
Bisphenol A-d16	BPA-d16	368	386	71 ± 17

Table S3. GC/MSD conditions for analyzing persistent toxic substances, including polychlorinated biphenyls (PCBs), polycyclic aromatic hydrocarbons (PAHs), styrene oligomers (SOs), and alkylphenols (APs).

Instrument	**Agilent 7890B GC / 5977B MSD**	
Column	DB-5ms (30 m × 250 μm × 0.25 μm)	
Gas flow	1 mL min^{-1} He	
Injection mode	Splitless	
Injection volume	1 μL	
Oven temperature program	PCBs	60 °C (hold 1 min) → 5 °C min^{-1} to 140 °C (hold 1 min) → 30 °C min^{-1} to 200 °C (hold 1 min) → 4 °C min^{-1} to 250 °C (hold 5 min) → 10 °C min^{-1} to 300 °C (hold 1 min)
	PAHs (t-PAHs and e-PAHs)	60 °C (hold 2 min) → 6 °C min^{-1} to 300 °C (hold 13 min)
	SOs	60 °C (hold 2 min) → 6 °C min^{-1} to 300 °C (hold 3 min)
	APs	60 °C (hold 5 min) → 10 °C min^{-1} to 100 °C → 20 °C min^{-1} to 300 °C (hold 6 min)

Table S4. Concentrations of polychlorinated biphenyls (PCBs) in sediments of the Yellow Sea.

Sites	PCBs (ng g^{-1} OC)															
	8	**28**	**52**	**49**	**44**	**37**	**74**	**70**	**66**	**60**	**101**	**99**	**87**	**77**	**82**	**118**
N3201	1.0	15	0.72	0.88	-	3.0	-	0.62	0.55	-	0.72	-	0.52	-	-	0.97
N3203	3.0	39	1.6	11	3.6	2.0	1.3	0.75	1.5	1.1	0.84	-	-	1.1	0.80	0.55
N3205	5.1	22	1.1	3.3	2.3	2.3	0.98	0.83	-	1.7	-	0.61	-	-	0.61	0.55
N3207	6.8	70	2.7	8.5	23	9.9	3.4	1.7	0.66	3.0	2.7	-	1.3	3.4	1.2	0.73
N3209	10	27	0.61	3.2	0.52	67	2.1	1.3	0.85	2.0	1.1	0.83	1.9	2.4	0.63	0.86
N3211	9.7	47	1.4	13	2.0	2.0	0.68	0.80	0.72	1.6	1.6	1.2	1.1	1.3	-	1.2
N3301	100	46	2.6	5.4	5.0	110	1.3	-	1.9	3.2	1.2	1.1	5.3	3.3	1.8	1.2
N3305	27	25	0.78	0.67	1.5	4.0	2.2	0.80	-	2.3	1.2	-	1.0	-	0.84	-
N3307	2.0	3.6	-	1.6	0.9	2.0	-	0.66	-	-	0.64	1.5	0.97	0.64	0.97	0.66
N3309	14	100	3.9	16	1.2	20	8.7	1.4	1.3	8.1	2.1	0.63	1.3	2.1	1.3	2.3
N3311	410	76	2.8	2.7	7.3	7.1	6.0	3.6	0.69	1.3	1.4	0.97	2.8	2.5	3.9	3.2
N3313	500	150	4.4	24	18	12	7.1	0.97	-	9.9	2.3	2.4	1.1	1.4	1.1	5.7
N3401	5.1	49	1.3	11	19	8.0	1.7	5.0	2.0	1.3	2.2	0.65	0.74	1.9	0.86	1.5
N3404	16	160	4.5	28	14	14	9.6	8.0	3.3	4.5	3.2	2.7	2.6	0.88	1.3	2.1
N3407	150	19	1.2	0.65	1.2	70	1.8	1.3	1.5	0.58	1.0	1.3	1.1	2.1	0.84	1.3
N3411	7.8	24	0.68	4.7	1.4	44	1.6	1.8	1.5	0.52	-	-	-	1.5	0.70	1.2
N3413	5.2	25	2.2	2.8	1.3	2.4	0.91	2.8	1.6	1.5	18	5.9	22	2.7	9.5	98
N3415	4.4	33	4.7	12	3.6	1.9	0.85	0.90	0.67	2.9	-	-	1.3	-	2.3	0.9
N3417	12	170	8.4	13	11	30	12	8.7	6.1	13	2.3	1.6	2.1	5.2	21	1.5
N3419	39	180	6.6	14	6.3	430	14	16	1.6	11	2.3	4.7	2.5	2.5	8.7	11
N3503	3.4	66	3.1	4.7	3.2	6.3	1.9	-	0.69	3.8	0.56	0.86	2.1	1.2	1.4	1.2
N3507	7.3	88	3.5	11	15	5.3	3.5	2.5	1.3	0.95	2.2	2.4	1.5	2.5	2.5	3.0
N3509	4.3	94	3.6	24	25	4.3	4.0	6.8	1.2	1.6	0.61	-	1.9	3.3	0.90	3.6
N3511	6.1	51	-	10	1.9	3.5	1.9	2.6	0.54	1.3	0.70	-	1.2	0.83	8.8	2.3
N3513	2.6	44	7.8	7.4	13	4.1	1.9	2.6	0.50	-	0.86	0.70	-	1.2	-	-
N3515	7.6	15	0.59	2.7	1.3	0.81	-	-	0.60	-	-	-	0.96	-	0.56	0.81
N3517	3.2	14	0.94	3.4	0.65	1.8	0.52	0.63	0.54	-	1.4	0.82	1.1	1.5	-	1.4
N3519	210	72	5.5	17	7.9	14	5.6	2.3	1.1	4.6	1.3	1.8	3.5	3.3	12	3.8
N3605	58	420	31	85	9.7	53	21	7.5	6.0	25	9.9	6.3	9.0	2.8	4.2	2.9
N3608	200	27	1.7	4.5	2.5	2.8	0.86	2.6	1.8	-	1.3	1.4	1.1	-	1.3	2.6
N3611	2.5	17	1.8	12	2.6	1.7	0.81	1.1	0.95	0.84	-	0.53	0.91	-	1.9	0.60
N3615	1.6	26	0.51	15	4.8	2.3	1.3	-	1.1	0.75	1.6	0.74	0.73	0.69	0.59	-
N3706	46	290	14	36	62	66	25	3.2	5.2	46	15	3.0	2.4	7.5	72	45
N3709	73	460	17	34	68	43	18	14	5.6	7.1	5.8	2.8	3.1	6.8	22	17
N3711	14	82	5.2	34	35	8.4	5.0	7.5	1.2	1.9	1.6	1.7	2.1	0.99	12	1.5

- : Below detection limits.

Table S4. (Continue).

Sites	PCBs (ng g^{-1} OC)																
	114	**153**	**105**	**179**	**138**	**158**	**126**	**166**	**187**	**183**	**128**	**156**	**180**	**169**	**170**	**189**	**Total**
N3201	0.74	24	-	1.6	-	-	-	-	-	2.4	0.82	0.59	1.3	-	1.1	-	60
N3203	-	61	0.87	-	0.68	-	0.64	-	1.6	-	1.2	1.8	-	1.0	-	1.1	140
N3205	0.81	3.9	0.66	-	-	-	1.2	-	1.7	1.5	-	-	-	0.57	-	-	56
N3207	3.9	25	1.0	1.2	-	0.59	3.4	0.91	1.9	0.95	4.3	-	1.6	-	2.0	-	190
N3209	1.9	25	1.6	2.4	1.0	1.0	1.8	0.58	0.95	1.4	1.5	1.5	0.91	0.70	0.75	-	170
N3211	1.9	73	1.2	-	1.0	0.75	1.1	0.82	1.6	1.7	-	1.3	-	-	1.4	0.62	170
N3301	1.5	45	2.1	4.4	0.74	-	3.7	-	3.5	1.8	2.0	-	5.9	0.98	0.93	0.81	370
N3305	0.96	14	2.5	2.3	0.61	-	1.3	0.54	2.6	0.90	1.3	0.94	0.88	-	-	-	98
N3307	0.59	18	1.1	-	-	-	-	-	3.1	4.2	-	-	-	0.90	1.0	4.1	53
N3309	3.9	140	4.5	-	0.56	-	2.6	0.62	0.60	-	1.3	1.3	0.96	1.3	3.2	2.1	350
N3311	3.6	19	4.9	0.90	-	-	2.1	0.60	-	-	1.7	1.6	-	2.0	1.0	-	570
N3313	1.5	160	11	-	-	1.3	6.0	0.78	1.5	1.6	4.1	1.6	0.91	1.9	2.4	2.1	940
N3401	0.94	93	7.2	1.41	0.55	0.55	2.9	0.80	-	0.80	2.7	1.9	-	1.2	-	0.60	230
N3404	3.3	75	8.3	-	0.89	1.5	94	0.99	2.8	-	0.66	2.6	0.55	3.6	-	1.6	470
N3407	0.92	41	-	-	0.98	-	2.7	-	1.3	2.6	-	-	2.8	1.2	-	-	310
N3411	-	28	0.84	0.55	0.60	-	1.3	0.78	1.3	0.87	0.81	1.3	2.1	1.3	-	-	130
N3413	4.1	180	71	3.1	24	76	1.5	2.0	8.0	5.4	74	48	31	-	46	1.9	780
N3415	-	40	0.81	-	-	-	0.99	1.2	-	-	0.84	0.81	-	1.4	1.8	-	120
N3417	10	120	4.7	5.3	1.0	1.0	3.9	1.2	4.5	3.0	14	18	2.3	3.3	1.7	3.0	510
N3419	3.1	76	7.5	3.2	1.0	3.1	4.2	2.5	1.2	1.2	5.6	9.8	2.1	6.5	6.2	2.0	880
N3503	1.1	49	1.9	1.3	0.60	0.66	3.2	0.64	3.3	2.7	4.5	1.5	0.62	1.4	-	2.2	180
N3507	2.3	92	2.3	0.69	1.1	-	2.6	0.92	7.1	3.7	2.9	1.4	1.4	1.1	0.79	-	270
N3509	-	59	2.2	0.84	-	-	2.9	1.7	0.77	-	5.8	1.4	0.93	4.2	2.1	1.3	260
N3511	1.4	21	1.4	1.7	0.69	-	0.70	-	1.7	2.7	1.6	1.5	1.1	2.4	1.6	-	130
N3513	1.1	33	0.96	1.1	-	0.79	-	-	1.1	-	0.99	4.9	-	1.2	-	1.2	140
N3515	-	2.7	-	-	-	-	1.0	-	-	-	0.72	-	0.51	-	-	-	42
N3517	0.63	47	-	0.81	-	-	0.57	0.75	-	-	0.58	0.84	-	0.97	-	0.71	86
N3519	2.7	57	3.5	-	-	0.66	3.2	0.84	-	0.87	1.8	1.7	-	3.5	1.1	1.6	450
N3605	7.6	150	20	1.3	0.88	2.4	18	12	1.7	2.6	6.4	36	4.0	4.7	7.8	5.8	1000
N3608	-	21	2.2	-	1.7	0.58	1.6	0.51	-	0.73	1.0	1.7	0.86	0.77	0.79	2.5	290
N3611	1.9	7.9	1.6	-	-	-	0.89	0.52	-	-	0.75	0.57	-	0.92	-	-	62
N3615	1.5	25	0.97	-	0.88	-	0.88	-	0.86	-	0.83	4.9	-	2.0	0.73	1.1	100
N3706	28	470	22	0.53	1.4	1.4	23	0.84	2.0	1.4	5.2	35	5.8	8.2	3.6	2.4	1300
N3709	11	180	20	6.8	4.6	2.3	19	4.5	1.5	0.75	25	3.6	4.4	1.4	0.97	2.6	1100
N3711	3.6	110	3.2	3.7	0.53	0.5	6.0	1.6	-	-	4.0	4.6	-	4.7	3.2	2.8	370

- : Below detection limits.

Table S5. Concentrations of traditional polycyclic aromatic hydrocarbons (t-PAHs) in sediments of the Yellow Sea.

Sites	t-PAHs (ng g^{-1} OC)															
	Acl	Ace	Flu	Phe	Ant	Fl	Py	BaA	Chr	BbF	BkF	BaP	IcdP	DbahA	BghiP	Total
N3201	20	79	380	900	1200	490	270	94	150	110	170	67	370	160	370	4800
N3203	37	130	280	1000	94	800	520	190	300	220	270	120	570	180	630	5400
N3205	24	84	390	1000	95	860	460	200	270	210	280	140	570	170	620	5400
N3207	65	120	310	1200	150	2400	3000	1000	1000	900	1200	1500	1700	410	1900	17000
N3209	14	46	200	380	46	400	200	120	160	120	150	110	310	120	400	2800
N3211	55	190	470	1400	95	730	400	180	260	150	180	150	440	120	600	5400
N3301	22	88	630	1100	130	600	290	130	210	140	210	14	380	98	420	4500
N3305	13	41	140	410	55	530	260	150	220	150	240	76	350	80	370	3100
N3307	54	270	1000	2200	120	970	520	200	310	210	310	170	600	170	700	7800
N3309	21	99	86	310	68	480	260	150	210	130	210	94	380	93	470	3100
N3311	15	35	49	170	35	230	130	590	94	140	65	41	170	37	200	1500
N3313	42	76	130	440	97	630	410	230	310	170	270	140	490	130	670	4200
N3401	58	220	410	1300	78	700	380	140	220	140	140	17.3	320	100	400	4600
N3404	23	54	180	380	130	590	300	120	160	87	110	36	150	47	240	2600
N3407	12	41	29	92	16	110	65	30	40	22	5.2	8.4	76	71	100	710
N3411	40	100	480	1300	96	990	510	190	310	200	280	68	450	130	530	5700
N3413	40	83	370	960	100	940	500	210	330	230	360	120	600	160	700	5700
N3415	58	150	340	1200	110	870	560	220	310	210	330	80	580	140	640	5800
N3417	46	120	290	860	100	640	410	140	250	110	100	130	260	210	430	4100
N3419	30	43	46	160	27	65	67	37	35	24	21	18	100	140	110	920
N3503	31	80	240	890	130	1200	670	230	270	160	260	170	430	150	510	5400
N3507	45	180	380	1100	73	400	250	61	120	82	62	9.9	170	89	170	3200
N3509	58	140	310	1100	190	1100	680	200	360	270	390	130	600	130	740	6500
N3511	58	140	290	1100	140	1200	810	500	560	1000	650	510	990	190	1300	9500
N3513	50	100	230	1000	120	1200	820	310	440	370	560	270	900	210	1000	7600
N3515	7.5	14	23	94	14	110	60	22	39	18	10	1.2	60	21	81	570
N3517	32	65	240	800	92	770	450	140	240	180	220	77	430	120	560	4400
N3519	27	55	89	380	680	560	310	140	220	110	210	66	330	83	390	3000
N3605	100	370	860	2800	220	1300	790	1800	500	230	300	140	430	140	570	11000
N3608	34	42	130	560	55	950	400	180	330	250	350	130	560	160	650	4800
N3611	67	120	240	1400	210	2300	1400	550	600	520	750	400	1400	280	1400	12000
N3615	68	110	210	1100	140	1200	800	320	390	280	460	230	950	210	980	7500
N3706	30	150	140	310	46	180	180	410	120	48	17	15	150	49	220	2100
N3709	62	160	270	740	130	600	380	150	260	150	220	75	250	6.6	320	3800
N3711	100	260	540	1900	2600	1300	1000	220	420	570	1200	89	510	150	640	12000

Table S6. Concentrations of emerging polycyclic aromatic hydrocarbons (e-PAHs) in sediments of the Yellow Sea.

Sites	e-PAHs (ng g^{-1} OC)								
	2MA	9EP	BBNF	BBNT	5MBA	BCP	BJF	BEP	Total
N3201	16	15	52	31	2.4	0.50	150	270	540
N3203	325	20	71	73	8.3	13	330	540	1100
N3205	26	18	75	64	16	6.7	290	500	1000
N3207	54	48	220	290	130	36	1200	2600	4500
N3209	100	34	39	37	22	9.6	160	300	700
N3211	290	84	81	71	5.2	12	280	490	1300
N3301	10	58	62	41	15	9.7	220	360	780
N3305	8.9	33	61	36	5.8	3.6	230	360	740
N3307	260	58	94	55	39	6.6	320	610	1400
N3309	12	53	65	51	16	11	230	380	820
N3311	54	12	32	21	6.0	0.5	140	160	420
N3313	210	58	85	64	23	18	310	520	1300
N3401	250	94	58	60	10	16	190	300	970
N3404	91	38	71	33	4.3	13	140	200	590
N3407	24	13	17	4.3	8.9	0.90	35	74	180
N3411	28	59	80	57	37	4.4	300	520	1100
N3413	270	67	98	58	5.4	4.8	350	590	1500
N3415	35	83	77	74	48	12	350	550	1200
N3417	25	75	64	58	19	16	150	320	730
N3419	98	31	41	57	17	2.1	24	3.2	270
N3503	170	61	91	24	12	12	290	460	1100
N3507	180	8.1	33	29	4.6	35	100	140	530
N3509	330	92	94	35	36	21	410	610	1600
N3511	330	89	110	68	7.8	16	1000	1200	2900
N3513	37	87	110	23	53	12	490	860	1700
N3515	27	3.2	15	7.1	2.4	1.6	37	66	160
N3517	250	49	69	48	17	8.3	200	450	1100
N3519	120	30	73	45	7.9	7.1	200	360	850
N3605	700	180	73	87	16	16	320	430	1800
N3608	190	45	99	51	16	4.3	280	560	1200
N3611	450	97	160	34	62	11	680	1200	2700
N3615	49	85	100	27	34	36	420	840	1600
N3706	150	26	32	79	27	20	66	30	430
N3709	300	25	24	79	12	26	150	250	870
N3711	460	120	95	17	13	28	570	590	1900

Table S7. Concentrations of styrene oligomers (SOs) in sediments of the Yellow Sea.

Sites	SOs (ng g^{-1} OC)										
	SD1	SD2	SD3	SD4	ST1	ST2	ST3	ST4	ST5	ST7	Total
N3201	12	4.6	350	15	22	130	130	93	1100	130	2000
N3203	68	32	440	300	85	230	320	250	220	550	2500
N3205	12	6.9	260	19	11	50	50	29	190	120	740
N3207	74	35	680	370	260	780	780	780	1100	570	5400
N3209	9.6	4.7	420	26	13	130	130	19	470	190	1400
N3211	120	66	730	540	210	418	670	570	550	750	4600
N3301	31	19	890	50	25	417	450	47	18007	530	4200
N3305	6.9	3.4	340	20	8.5	20	27	110	97	280	900
N3307	31	12	1300	46	28	46	51	66	290	700	2600
N3309	27	7.9	490	47	77	170	220	150	190	230	1600
N3311	27	28	590	190	77	210	330	180	250	130	2000
N3313	42	26	820	100	120	280	410	310	420	330	2800
N3401	120	67	1000	620	190	440	610	480	440	620	4600
N3404	35	10	85	77	71	190	260	310	470	320	1800
N3407	7.9	4.3	800	21	17	57	26	38	140	250	1400
N3411	16	6.4	270	23	11	25	29	73	44	230	730
N3413	17	11	480	29	63	170	240	300	410	260	2000
N3415	61	28	200	260	100	260	280	310	320	630	2500
N3417	76	50	390	610	410	850	1300	590	890	580	5700
N3419	93	82	250	620	280	680	1000	540	690	490	4800
N3503	69	37	570	340	110	240	340	270	240	340	2600
N3507	24	14	920	80	83	220	160	100	230	560	2400
N3509	44	48	460	410	220	420	790	420	450	850	4100
N3511	60	35	150	340	210	1100	660	2200	2900	480	8200
N3513	38	17	180	200	180	630	580	300	310	320	2800
N3515	3.8	1.8	19	7.9	9.5	47	14	88	130	70	390
N3517	12	3.9	33	22	17	40	18	26	86	100	360
N3519	26	9.7	620	36	55	260	140	670	1200	350	3300
N3605	270	130	630	1700	360	830	1000	760	820	1900	8400
N3608	12	5.1	44	19	27	21	55	65	53	190	490
N3611	35	18	180	180	120	200	310	210	190	540	2000
N3615	3.4	1.5	17	7.0	8.4	41	13	78	110	62	340
N3706	180	110	7600	1600	300	1100	750	1700	960	11000	25000
N3709	130	87	7100	1200	190	620	420	1100	640	8200	20000
N3711	18	24	1700	120	97	110	130	210	750	3200	6400

Table S8. Concentrations of alkylphenols (APs) in sediments of the Yellow Sea.

Sites	APs (ng g^{-1} OC)						
	t-OP	NPs	t-OP1EO	NP1EOs	t-OP2EO	NP2EOs	Total APs
N3201	15	27	17	120	20	150	350
N3203	21	33	19	110	38	450	670
N3205	17	33	27	200	23	310	610
N3207	21	48	33	290	78	760	1200
N3209	23	43	22	390	2100	1200	3800
N3211	43	78	54	360	85	1100	1700
N3301	32	90	62	680	110	850	1800
N3305	19	41	38	270	72	380	820
N3307	22	42	29	420	160	480	1200
N3309	16	37	36	210	12	340	650
N3311	29	43	28	160	17	400	680
N3313	52	50	43	300	55	610	1100
N3401	37	44	54	61	110	390	700
N3404	4.1	4.3	3.9	16	3.5	15	47
N3407	39	13	56	170	36	110	420
N3411	12	24	190	48	41	74	380
N3413	24	8.9	120	160	34	140	480
N3415	20	30	21	97	17	83	270
N3417	43	39	51	160	40	160	490
N3419	89	120	83	190	65	160	700
N3503	22	39	31	140	58	160	450
N3507	53	79	68	280	94	710	1300
N3509	24	29	24	140	40	380	630
N3511	18	20	17	75	27	82	240
N3513	16	14	15	69	26	85	220
N3515	12	22	16	76	18	46	190
N3517	14	19	32	70	24	98	260
N3519	19	41	19	71	110	120	380
N3605	390	160	140	570	250	660	2200
N3608	21	52	32	280	130	180	710
N3611	8.8	17	16	95	62	100	300
N3615	7.7	20	19	110	11	95	260
N3706	58	120	140	520	120	500	1500
N3709	89	94	95	360	94	410	1100
N3711	63	150	71	250	67	190	790

Table S9. Concentrations of heavy metals in sediments of the Yellow Sea.

Sites	Concentrations of metals (μg g^{-1} dw)																
	Mn	**Li**	**V**	**Cr**	**Co**	**Ni**	**Cu**	**Zn**	**As**	**Sr**	**Mo**	**Ag**	**Cd**	**Sn**	**Sb**	**Pb**	**Hg**
N3201	670	46	78	66	11	29	12	74	670	330	0.25	0.04	0.10	2.4	0.50	17	0.023
N3203	740	49	82	70	13	31	13	77	740	250	0.32	0.04	0.09	2.5	0.55	20	0.019
N3205	500	62	110	87	16	41	20	97	500	150	0.40	0.05	0.10	3.2	0.75	23	0.020
N3207	680	39	78	60	12	28	14	65	680	140	0.37	0.05	0.09	2.3	0.57	19	0.015
N3209	840	35	110	82	13	29	13	68	840	150	0.38	0.07	0.12	2.6	0.64	19	0.015
N3211	590	29	74	56	11	24	10	54	590	120	0.35	0.05	0.08	2.0	0.51	19	0.011
N3301	700	23	49	39	8.8	18	5.3	45	700	320	0.24	0.03	0.06	1.5	0.38	14	0.013
N3305	700	50	83	66	13	31	14	76	700	190	0.31	0.05	0.09	2.7	0.60	20	0.017
N3307	530	37	70	57	11	25	12	60	530	150	0.30	0.05	0.10	2.2	0.60	19	0.014
N3309	860	36	98	91	13	28	13	68	860	160	0.46	0.06	0.10	2.5	0.63	19	0.015
N3311	820	41	97	69	14	31	15	72	820	170	0.44	0.06	0.12	2.6	0.67	20	0.016
N3313	780	33	93	83	12	26	12	60	780	170	0.41	0.06	0.13	2.4	0.65	16	0.014
N3401	490	31	44	35	7.5	15	6.9	43	490	300	0.21	0.04	0.06	1.3	0.37	17	0.010
N3404	660	35	57	47	10	18	8.7	49	660	370	0.25	0.05	0.08	1.7	0.41	20	0.010
N3407	340	27	46	38	7.7	16	8.4	43	340	130	0.19	0.04	0.07	1.5	0.37	18	0.012
N3411	660	47	80	63	12	29	15	71	660	110	0.34	0.06	0.09	2.5	0.64	20	0.017
N3413	470	46	82	64	12	30	16	71	470	100	0.31	0.06	0.10	2.4	0.70	21	0.019
N3415	690	51	93	74	13	33	18	79	690	120	0.46	0.07	0.12	2.8	0.83	22	0.019
N3417	780	31	63	53	9.7	23	10	51	780	160	0.30	0.05	0.09	1.9	0.58	13	0.012
N3419	600	22	65	58	8.6	19	6.9	42	600	170	0.23	0.05	0.10	1.8	0.47	12	0.007
N3503	450	48	72	61	11	24	12	68	450	92	0.31	0.07	0.10	2.6	0.56	21	0.015
N3507	400	20	38	40	6.5	13	6.1	34	400	98	0.27	0.05	0.09	1.4	0.35	19	0.007
N3509	310	46	73	56	11	26	15	68	310	93	0.32	0.09	0.15	2.4	0.71	22	0.018
N3511	310	48	80	63	12	29	18	72	310	92	0.29	0.09	0.13	2.6	0.75	22	0.019
N3513	460	62	110	86	15	39	23	95	460	77	0.39	0.09	0.12	3.3	0.88	25	0.025
N3515	580	66	120	88	16	41	24	100	580	88	0.45	0.08	0.12	3.4	0.90	25	0.025
N3517	950	57	110	83	15	39	23	92	950	84	0.66	0.07	0.11	3.3	0.90	24	0.023
N3519	1100	37	69	56	11	26	17	61	1100	110	0.75	0.07	0.10	2.2	0.91	20	0.016
N3605	150	8.5	18	16	3.3	4.9	2.5	15	150	64	0.11	0.04	0.03	0.75	0.21	19	0.004
N3608	370	33	57	49	8.8	20	14	54	370	83	0.39	0.09	0.08	4.0	0.57	22	0.019
N3611	690	66	120	89	16	42	30	110	690	62	0.46	0.10	0.15	4.2	1.1	29	0.037
N3615	1200	73	130	95	18	48	31	110	1200	72	0.65	0.08	0.14	3.7	1.1	28	0.034
N3706	300	11	22	15	4.2	6.0	2.8	20	300	88	0.36	0.03	0.03	0.87	0.26	22	0.004
N3709	350	12	26	20	5.2	7.8	3.4	22	350	79	0.24	0.04	0.07	1.2	0.32	19	0.005
N3711	590	24	46	40	7.5	16	9.4	39	590	150	0.49	0.07	0.09	1.7	0.73	16	0.013

Table S10. Enrichment factors of metals in sediments of the Yellow Sea.

Sites	Enrichment factor																
	Mn	Li	V	Cr	Co	Ni	Cu	Zn	As	Sr	Mo	Ag	Cd	Sn	Sb	Pb	Hg
N3201	0.9	1.2	0.9	0.8	0.8	0.9	0.5	1.0	0.5	1.5	0.3	0.5	0.9	0.6	0.5	0.6	0.7
N3203	0.9	1.2	0.8	0.8	0.8	0.9	0.5	0.9	0.5	1.0	0.3	0.4	0.7	0.6	0.5	0.6	0.5
N3205	0.5	1.3	0.9	0.9	0.9	1.0	0.7	1.0	0.7	0.5	0.3	0.5	0.7	0.7	0.6	0.6	0.5
N3207	0.9	1.0	0.9	0.8	0.8	0.9	0.6	0.9	0.9	0.6	0.4	0.6	0.8	0.6	0.6	0.7	0.4
N3209	1.2	0.9	1.2	1.1	0.9	0.9	0.6	0.9	0.9	0.7	0.4	0.9	1.1	0.7	0.7	0.7	0.5
N3211	1.0	0.9	1.0	0.9	0.9	0.9	0.5	0.9	0.9	0.7	0.5	0.8	0.9	0.7	0.7	0.8	0.4
N3301	1.2	0.8	0.7	0.6	0.8	0.7	0.3	0.8	0.8	1.8	0.3	0.5	0.7	0.5	0.5	0.6	0.5
N3305	0.8	1.1	0.7	0.7	0.7	0.8	0.5	0.8	0.6	0.7	0.3	0.5	0.6	0.6	0.5	0.6	0.4
N3307	0.7	1.0	0.8	0.7	0.7	0.8	0.5	0.8	0.8	0.7	0.3	0.6	0.9	0.6	0.7	0.7	0.4
N3309	1.1	0.9	1.0	1.1	0.8	0.8	0.5	0.8	0.8	0.7	0.5	0.7	0.8	0.6	0.6	0.6	0.4
N3311	1.0	1.0	0.9	0.8	0.8	0.9	0.6	0.8	0.8	0.7	0.4	0.7	0.9	0.6	0.6	0.6	0.4
N3313	1.0	0.9	1.0	1.0	0.8	0.8	0.5	0.8	0.8	0.7	0.4	0.7	1.1	0.6	0.7	0.6	0.4
N3401	0.8	1.0	0.6	0.6	0.6	0.6	0.4	0.7	0.7	1.7	0.3	0.6	0.7	0.5	0.5	0.8	0.4
N3404	0.9	1.0	0.7	0.6	0.7	0.6	0.4	0.7	0.9	1.7	0.3	0.7	0.7	0.5	0.5	0.7	0.3
N3407	0.6	1.0	0.7	0.6	0.7	0.7	0.5	0.8	0.7	0.7	0.3	0.7	0.8	0.5	0.5	0.8	0.5
N3411	0.9	1.3	0.9	0.8	0.8	0.9	0.7	1.0	0.7	0.5	0.4	0.8	0.8	0.7	0.7	0.7	0.5
N3413	0.6	1.2	0.9	0.8	0.8	0.9	0.7	0.9	0.7	0.4	0.3	0.7	0.9	0.7	0.8	0.7	0.6
N3415	0.8	1.1	0.8	0.8	0.7	0.9	0.7	0.9	0.7	0.4	0.4	0.7	0.9	0.6	0.8	0.6	0.5
N3417	1.0	0.8	0.7	0.6	0.6	0.7	0.4	0.7	0.7	0.7	0.3	0.6	0.8	0.5	0.6	0.5	0.3
N3419	0.9	0.7	0.8	0.8	0.6	0.7	0.3	0.6	0.9	0.8	0.3	0.7	1.0	0.5	0.6	0.5	0.2
N3503	0.8	1.7	1.1	1.0	1.0	1.0	0.7	1.2	1.0	0.5	0.5	1.2	1.2	1.0	0.8	1.0	0.6
N3507	1.0	1.0	0.8	1.0	0.8	0.8	0.5	0.9	1.1	0.8	0.6	1.2	1.5	0.7	0.7	1.2	0.4
N3509	0.5	1.5	1.0	0.8	0.9	1.0	0.8	1.1	0.6	0.5	0.4	1.4	1.6	0.8	0.9	0.9	0.6
N3511	0.4	1.3	0.9	0.8	0.8	0.9	0.8	1.0	0.6	0.4	0.3	1.1	1.2	0.7	0.8	0.8	0.6
N3513	0.6	1.6	1.2	1.1	1.0	1.2	1.0	1.2	0.7	0.3	0.4	1.1	1.0	0.9	0.9	0.8	0.7
N3515	0.5	1.1	0.8	0.7	0.7	0.8	0.7	0.9	0.5	0.2	0.3	0.6	0.7	0.6	0.6	0.6	0.5
N3517	1.1	1.3	1.0	0.9	0.9	1.1	0.9	1.1	0.9	0.3	0.6	0.8	0.8	0.8	0.9	0.7	0.6
N3519	1.9	1.3	1.0	0.9	1.0	1.1	1.0	1.1	1.1	0.6	1.1	1.2	1.2	0.8	1.3	0.9	0.6
N3605	0.4	0.4	0.3	0.3	0.4	0.3	0.2	0.4	0.7	0.5	0.2	0.9	0.5	0.4	0.4	1.2	0.2
N3608	0.5	0.8	0.6	0.6	0.5	0.6	0.6	0.7	0.6	0.3	0.4	1.0	0.7	1.0	0.6	0.7	0.5
N3611	0.5	1.0	0.7	0.6	0.6	0.7	0.7	0.8	0.4	0.2	0.3	0.7	0.7	0.6	0.7	0.6	0.6
N3615	1.0	1.2	0.9	0.7	0.7	0.9	0.8	0.9	0.6	0.2	0.4	0.6	0.8	0.6	0.8	0.6	0.6
N3706	0.6	0.4	0.3	0.3	0.4	0.3	0.2	0.4	0.8	0.5	0.5	0.5	0.4	0.3	0.4	1.1	0.2
N3709	0.5	0.4	0.3	0.3	0.4	0.3	0.2	0.3	0.4	0.4	0.3	0.5	0.6	0.4	0.4	0.7	0.2
N3711	1.1	0.9	0.7	0.7	0.7	0.7	0.6	0.7	1.0	0.9	0.8	1.3	1.2	0.7	1.2	0.8	0.5

0.0–1.0: not enriched, crustal contribution, 1.0–1.5: little enriched, > 1.5: anthropogenic or external burden.

Supplementary Figures

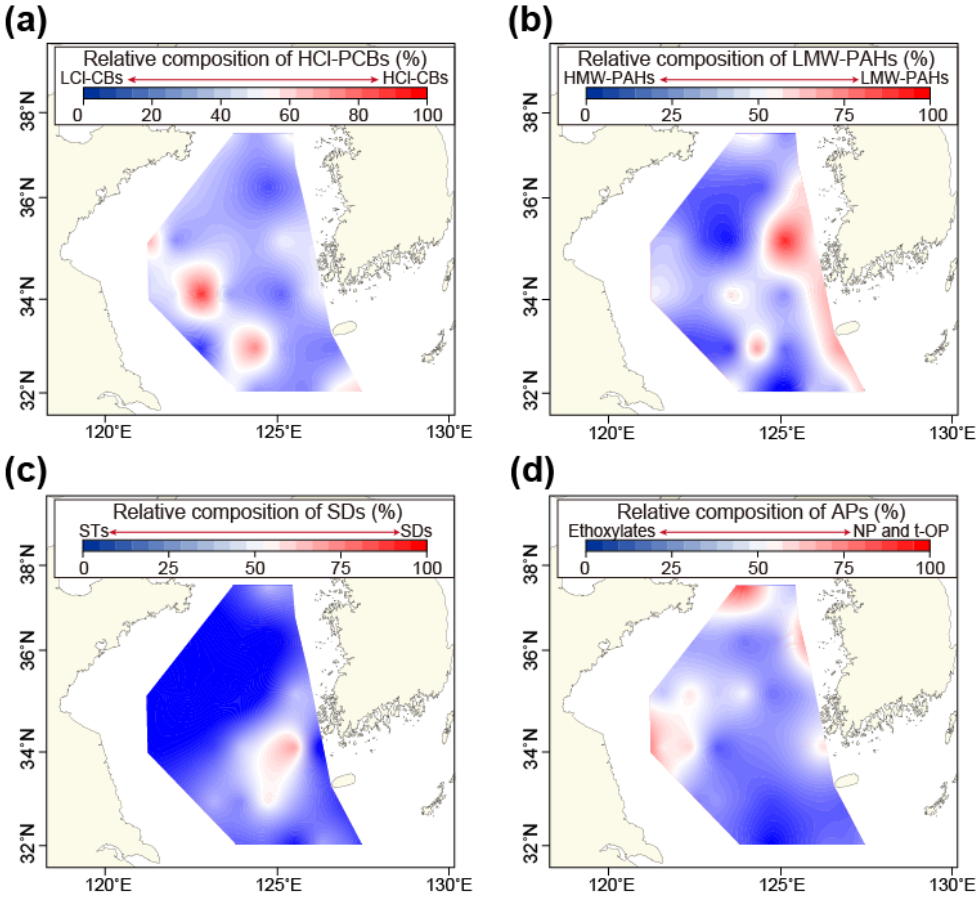

Fig. S1. Contour maps for relative compositions of **(a)** PCBs, **(b)** PAHs, **(c)** SOs, and **(d)** APs in sediments of the Yellow Sea.

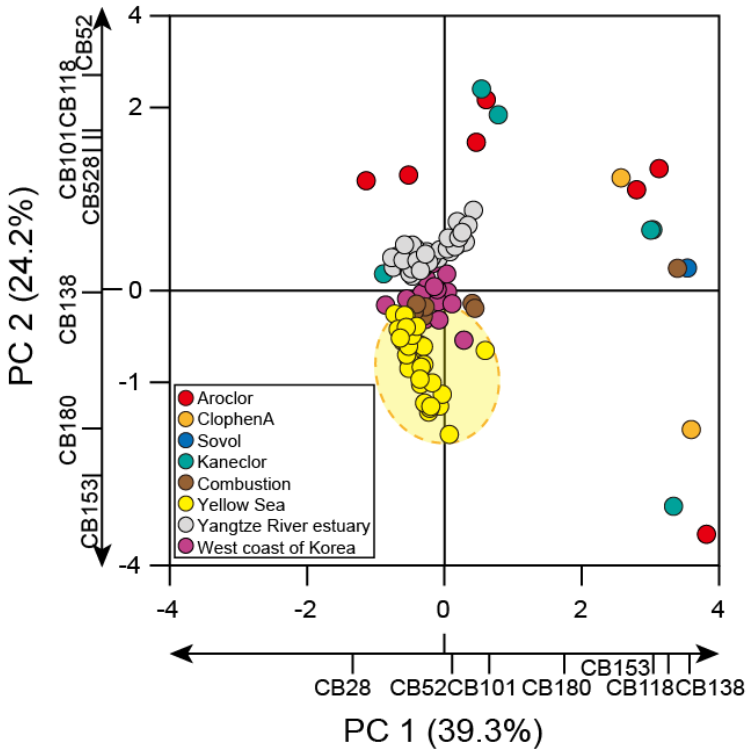

Fig. S2. Source identification of PCBs in sediments of the Yellow Sea using principal component analysis (PCA) [Source profiles of PCBs refer from Ikonomou et al. (2002) and Pedersen et al. (2015); PCBs profiles in Yangtze River sediments refer from Yang et al. (2012); PCBs profiles in sediments of the west coast of Korea refer from Kim et al. (2021)].

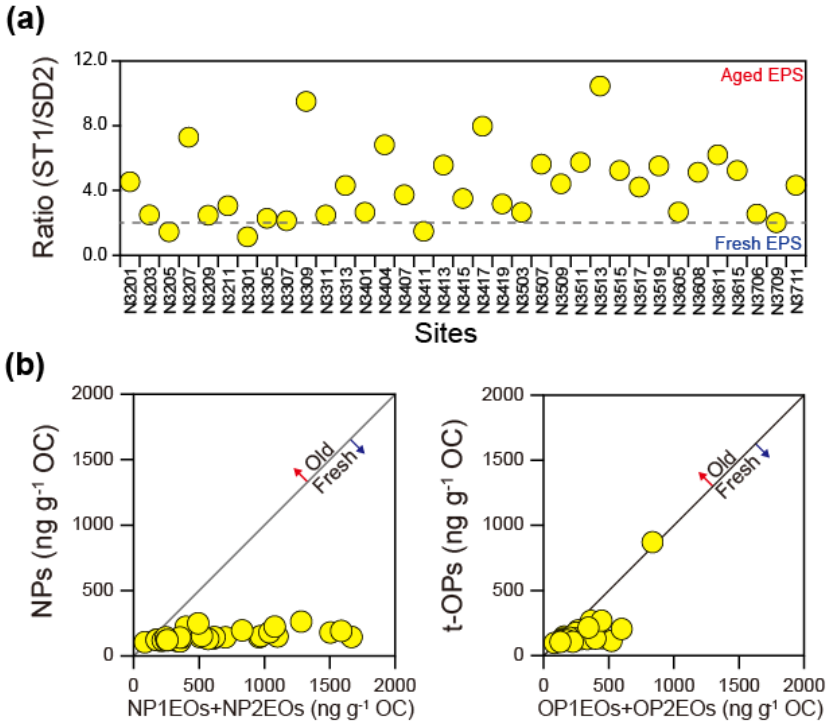

Fig. S3. Source identifications of **(a)** styrene oligomers, **(b)** nonylphenols, and octylphenols in sediments of the Yellow Sea using diagnostic ratios [diagnostic ratios refer from Isobe et al. (2001) and Tian et al. (2022)].

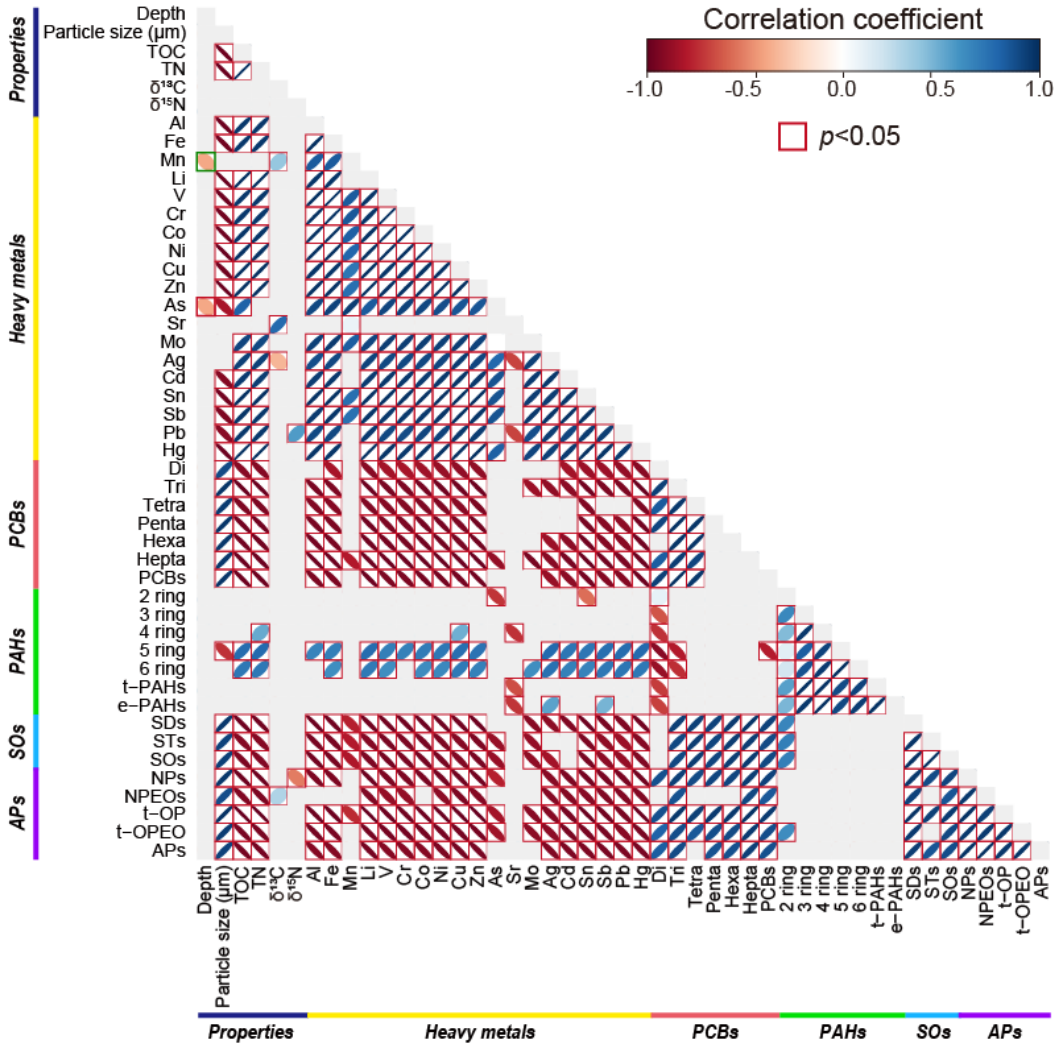

Fig. S4. Spearman's correlation relationships among mean grain size, organic carbon contents, metals, and PTSs concentrations in sediments of the Yellow Sea. Colored squares indicate the correlation coefficients of each factor.

References

An, Y., Hong, S., Yoon, S.J., Cha, J., Shin, K.-H., Khim, J.S., 2020. Current contamination status of traditional and emerging persistent toxic substances in the sediments of Ulsan Bay, South Korea. Mar. Pollut. Bull. 160, 111560. https://doi.org/10.1016/j.marpolbul.2020.111560.

Ikonomou, M., Sather, P., Oh, J.-E., Choi, W.-Y., Chang, Y.-S., 2002. PCB levels and congener patterns from Korean municipal waste incinerator stack emissions. Chemosphere 49(2), 205-216. https://doi.org/10.1016/S0045-6535(02)00102-9.

Isobe, T., Nishiyama, H., Nakashima, A., Takada, H., 2001. Distribution and behavior of nonylphenol, octylphenol, and nonylphenol monoethoxylate in Tokyo Metropolitan Area: Their association with aquatic particles and sedimentary distributions. Environ. Sci. Technol. 35(6), 1041-1049. https://doi.org/10.1021/es001250i.

Kim, Y., Hong, S., Lee, J., Yoon, S.J., An, Y., Kim, M.-S., Jeong, H.-D., Khim, J.S., 2021. Spatial distribution and source identification of traditional and emerging persistent toxic substances in the offshore sediment of South Korea. Sci. Total Environ. 789, 147996. https://doi.org/10.1016/j.scitotenv.2021.147996.

Pedersen, K.B., Lejon, T., Jensen, P.E., Ottosen, L.M., 2015. Chemometric analysis for pollution source assessment of harbour sediments in Arctic locations. Water, Air, Soil Pollut. 226(5), 150. https://doi.org/10.1007/s11270-015-2416-4.

Tian, Z., Kim, S.-K., Hyun, J.-H., 2020. Environmental distribution of styrene oligomers (SOs) coupled with their source characteristics: Tracing the origin of SOs in the environment. J. Hazard. Mater. 398, 122968. https://doi.org/10.1016/j.jhazmat.2020.122968.

Yang, H., Zhuo, S., Xue, B., Zhang, C., Liu, W., 2012. Distribution, historical trends and inventories of polychlorinated biphenyls in sediments from Yangtze River Estuary and adjacent East China Sea. Environ. Pollut. 169, 20-26. https://doi.org/https://doi.org/10.1016/j.envpol.2012.05.003.